NeuroImage 258 (2022) 119352

Contents lists available at ScienceDirect

NeuroImage

journal homepage: www.elsevier.com/locate/neuroimage

The human language effective connectome

Edmund T. Rolls [a,b,g,*], Gustavo Deco [c,d,e], Chu-Chung Huang [f], Jianfeng Feng [b,g]

[a] Oxford Centre for Computational Neuroscience, Oxford, UK
[b] Department of Computer Science, University of Warwick, Coventry CV4 7AL, UK
[c] Department of Information and Communication Technologies, Center for Brain and Cognition, Computational Neuroscience Group, Universitat Pompeu Fabra, Roc Boronat 138, Barcelona 08018, Spain
[d] Brain and Cognition, Pompeu Fabra University, Barcelona 08018, Spain
[e] Institució Catalana de la Recerca i Estudis Avançats (ICREA), Universitat Pompeu Fabra, Passeig Lluís Companys 23, Barcelona 08010, Spain
[f] Shanghai Key Laboratory of Brain Functional Genomics (Ministry of Education), School of Psychology and Cognitive Science, East China Normal University, Shanghai 200602, China
[g] Institute of Science and Technology for Brain Inspired Intelligence, Fudan University, Shanghai 200403, China

ARTICLE INFO

Keywords:
Language
Effective connectivity
Functional connectivity
Diffusion tractography
Broca's area
Semantic networks
Syntax

ABSTRACT

To advance understanding of brain networks involved in language, the effective connectivity between 26 cortical regions implicated in language by a community analysis and 360 cortical regions was measured in 171 humans from the Human Connectome Project, and complemented with functional connectivity and diffusion tractography, all using the HCP multimodal parcellation atlas. A (semantic) network (Group 1) involving inferior cortical regions of the superior temporal sulcus cortex (STS) with the adjacent inferior temporal visual cortex TE1a and temporal pole TG, and the connected parietal PGi region, has effective connectivity with inferior temporal visual cortex (TE) regions; with parietal PFm which also has visual connectivity; with posterior cingulate cortex memory-related regions; with the frontal pole, orbitofrontal cortex, and medial prefrontal cortex; with the dorsolateral prefrontal cortex; and with 44 and 45 for output regions. It is proposed that this system can build in its temporal lobe (STS and TG) and parietal parts (PGi and PGs) semantic representations of objects incorporating especially their visual and reward properties. Another (semantic) network (Group 3) involving superior regions of the superior temporal sulcus cortex and more superior temporal lobe regions including STGa, auditory A5, TPOJ1, the STV and the Peri-Sylvian Language area (PSL) has effective connectivity with auditory areas (A1, A4, A5, Pbelt); with relatively early visual areas involved in motion, e.g., MT and MST, and faces/words (FFC); with somatosensory regions (frontal opercular FOP, insula and parietal PF); with other TPOJ regions; and with the inferior frontal gyrus regions (IFJa and IFSp). It is proposed that this system builds semantic representations specialising in auditory and related facial motion information useful in theory of mind and somatosensory / body image information, with outputs directed not only to regions 44 and 45, but also to premotor 55b and midcingulate premotor cortex. Both semantic networks (Groups 1 and 3) have access to the hippocampal episodic memory system via parahippocampal TF. A third largely frontal network (Group 2) (44, 45, 47l; 55b; the Superior Frontal Language region SFL; and including temporal pole TGv) receives effective connectivity from the two semantic systems, and is implicated in syntax and speech output.

1. Introduction

Brain areas involved in language and the connectivity between them is a continuing topic of importance for understanding human brain function and in order to minimize language impairments during neurosurgery (Hickok and Poeppel, 2007; Rauschecker, 2012; DeWitt and Rauschecker, 2013; Bouchard et al., 2013; Hickok and Poeppel, 2015; Chang et al., 2015; Bornkessel-Schlesewsky et al., 2015; Ding et al., 2016; Milton et al., 2021). Part of the background is research on the auditory cortex in non-human primates (Rauschecker et al., 1995; Rauschecker, 1998; Kaas and Hackett, 2000). Earlier views of Wernicke's area and its connections with Broca's area (Geschwind, 1970) have now been re-evaluated (Coslett and Schwartz, 2018) to produce new views on Wernicke's area (DeWitt and Rauschecker, 2013; Binder, 2017), Broca's area (Kelly et al., 2010; Amunts and Zilles, 2012; Gajardo-Vidal et al., 2021), their evolutionary origins (Rauschecker, 2018b), and neuropsychological and neuroimaging investigations of language systems (Hagoort and Indefrey, 2014;

* Corresponding author at: Department of Computer Science, University of Warwick, Coventry CV4 7AL, UK.
E-mail address: Edmund.Rolls@oxcns.org (E.T. Rolls).

https://doi.org/10.1016/j.neuroimage.2022.119352.
Received 22 April 2022; Accepted 31 May 2022
Available online 2 June 2022.

Kemmerer, 2015; Hagoort, 2017; Friederici et al., 2017; Battistella et al., 2020). In more recent research utilising the Human Connectome Project multimodal parcellation (HCP-MMP) atlas (Glasser et al., 2016a), 157 task-based fMRI studies were analyzed to identify brain regions in the HCP-MMP atlas related to semantics based on categorization of visual words and objects, and auditory words and stories, and the following regions were identified as part of the semantic network: 44, 45, 55b, IFJa, 8C, p32pr, SFL, SCEF, 8BM, STSdp, STSvp, TE1p, PHT and PBelt, and were shown to be interconnected with tractography (Milton et al., 2021).

To advance understanding of language systems in the brain, we measured with Human Connectome Project data (Glasser et al., 2016b) the direct connections between 360 cortical regions in the HCP-MMP atlas using diffusion tractography; the functional connectivity between the regions using the correlation between the BOLD signals in resting state fMRI which provides evidence about the strength of interactions; and the effective connectivity which provides evidence about the strength and direction of the causal connectivity between pairs of the 360 cortical regions with a new Hopf algorithm (Rolls et al., 2022b, c). These measures were made between the 360 cortical regions in the Human Connectome Project multimodal parcellation atlas (HCP-MMP) (Glasser et al., 2016a). The HCP-MMP atlas provides the most detailed parcellation of the human cortical areas that we know, in that its 360 regions are defined using a combination of structural measures (cortical thickness and cortical myelin content), functional connectivity, and task-related fMRI (Glasser et al., 2016a). In this research, we performed community analysis on the 360 × 360 effective connectivity data, and identified a community of 26 cortical regions that included most of those or very similar regions noted above (Milton et al., 2021) related to language. We then performed analyses on the connections, functional connectivity, and effective connectivity of these 26 left hemisphere cortical regions with the 360 cortical regions in the HCP-MMP atlas (Glasser et al., 2016a).

Strengths of this investigation are that it utilised this HCP-MMP atlas (Glasser et al., 2016a); HCP data from the same set of 171 participants imaged at 7T in whom we could calculate the connections, functional connectivity, and effective connectivity; and that it utilised a method for effective connectivity measurement (Rolls et al., 2022b, c) between all 360 cortical regions investigated here. Measurement of effective connectivity is conceptually important, because it estimates the effect of one brain region on another (Valdes-Sosa et al., 2011; Bajaj et al., 2016), which is an essential component of our understanding of how the brain operates computationally (Rolls, 2016, 2021a). Moreover the effective connectivity instantiates a generative model, in that it is used to generate functional connectivity matrices at time t and $t + 2$ s, as described here.

2. Methods

2.1. Participants and data acquisition

All the data analyzed were from the Human Connectome project dataset (Glasser et al., 2016b), with the neuroimaging performed at 7T with 171 participants selected with data suitable for both resting state fMRI and diffusion tractography.

Multiband 7T resting state functional magnetic resonance images (rs-fMRI) of 184 individuals were obtained from the publicly available S1200 release (last updated: April 2018) of the Human Connectome Project (HCP) (Van Essen et al., 2013). Individual written informed content was obtained from each participant, and the scanning protocol was approved by the Institutional Review Board of Washington University in St. Louis, MO, USA (IRB #201204036).

Multimodal imaging was performed in a Siemens Magnetom 7T housed at the Center for Magnetic Resonance (CMRR) at the University of Minnesota in Minneapolis. For each participant, a total of four sessions of rs-fMRI were acquired, with oblique axial acquisitions alternated between phase encoding in a posterior-to-anterior (PA) direction in sessions 1 and 3, and an anterior-to-posterior (AP) phase encoding direction in sessions 2 and 4. Specifically, each rs-fMRI session was acquired using a multiband gradient-echo EPI imaging sequence. The following parameters were used: TR = 1000ms, TE = 22.2 ms, flip angle = 45°, field of view = 208 × 208, matrix = 130 × 130, 85 slices, voxel size = 1.6 × 1.6 × 1.6 mm^3, multiband factor = 5. The total scanning time for the rs-fMRI protocol was approximately 16 min with 900 volumes. Further details of the 7T rs-fMRI acquisition protocols are given in the HCP reference manual (https://humanconnectome.org/storage/app/media/documentation/s1200/HCP_S1200_Release_Reference_Manual.pdf).

The current investigation was designed to complement investigations of effective connectivity of the hippocampus (Rolls et al., 2022b) and posterior parietal cortex (Rolls et al., 2022d), and so the same 171 participants with data for all four sessions of rs-fMRI at 7T were used for the analyses described here (age 22–36 years, 66 males).

2.2. Data preprocessing

The preprocessing was performed by the HCP as described in Glasser et al. (2013), based on the updated 7T data pipeline (v3.21.0, https://github.com/Washington-University/HCPpipelines), including gradient distortion correction, head motion correction, image distortion correction, spatial transformation to the Montreal Neurological Institute space using one step spline resampling from the original functional images followed by intensity normalization. In addition, the HCP took an approach using ICA (FSL's MELODIC) combined with a more automated component classifier referred to as FIX (FMRIB's ICA-based X-noisifier) to remove non-neural spatiotemporal artefact (Smith et al., 2013; Salimi-Khorshidi et al., 2014; Griffanti et al., 2014). This step also used 24 confound timeseries derived from the motion estimation (6 rigid-body parameter timeseries, their backwards-looking temporal derivatives, plus all 12 resulting regressors squared (Satterthwaite et al., 2013) to minimise noise in the data. The preprocessing performed by the HCP also included boundary-based registration between EPI and T1w images, and brain masking based on FreeSurfer segmentation. The 'minimally preprocessed' rsfMRI data provided by the HCP 1200 release (rfMRI*hp2000_clean.dtseries) was used in this investigation. The preprocessed data is in the HCP grayordinates standard space and is made available in a surface-based CIFTI file for each participant. With the MATLAB script (cifti toolbox: https://github.com/Washington-University/cifti-matlab), we extracted and averaged the cleaned timeseries of all the grayordinates in each region of the HCP-MMP 1.0 atlas (Glasser et al., 2016a), which is a group-based parcellation defined in the HCP grayordinate standard space having 180 brain regions per hemisphere, and is a surface-based atlas provided in CIFTI format.

2.3. Brain atlas and region selection

To construct the effective connectivity for the regions of interest in this investigation with other parts of the human brain, we utilised the 7T resting state fMRI data from the HCP, and parcellated this with the surface based HCP-MMP atlas which has 360 cortical regions (Glasser et al., 2016a) reordered (Huang et al., 2022) as described in the Supplementary Material, named in Table S1, and illustrated in Figs. 1 and S1. Each region in this atlas was defined by a combination of multiple methods including cortical myelin, cortical thickness, functional connectivity, and task-related activations, with detailed descriptions of the boundaries of each region, and the task-related activations which are often important for the name provided for each region, provided in the Supplementary Material of Glasser et al. (2016a). We were able to use the same 171 participants for whom we also had performed diffusion tractography, as described in detail (Huang et al., 2021).

The cortical regions of interest in relation to language to be investigated were selected as follows using a community analysis of

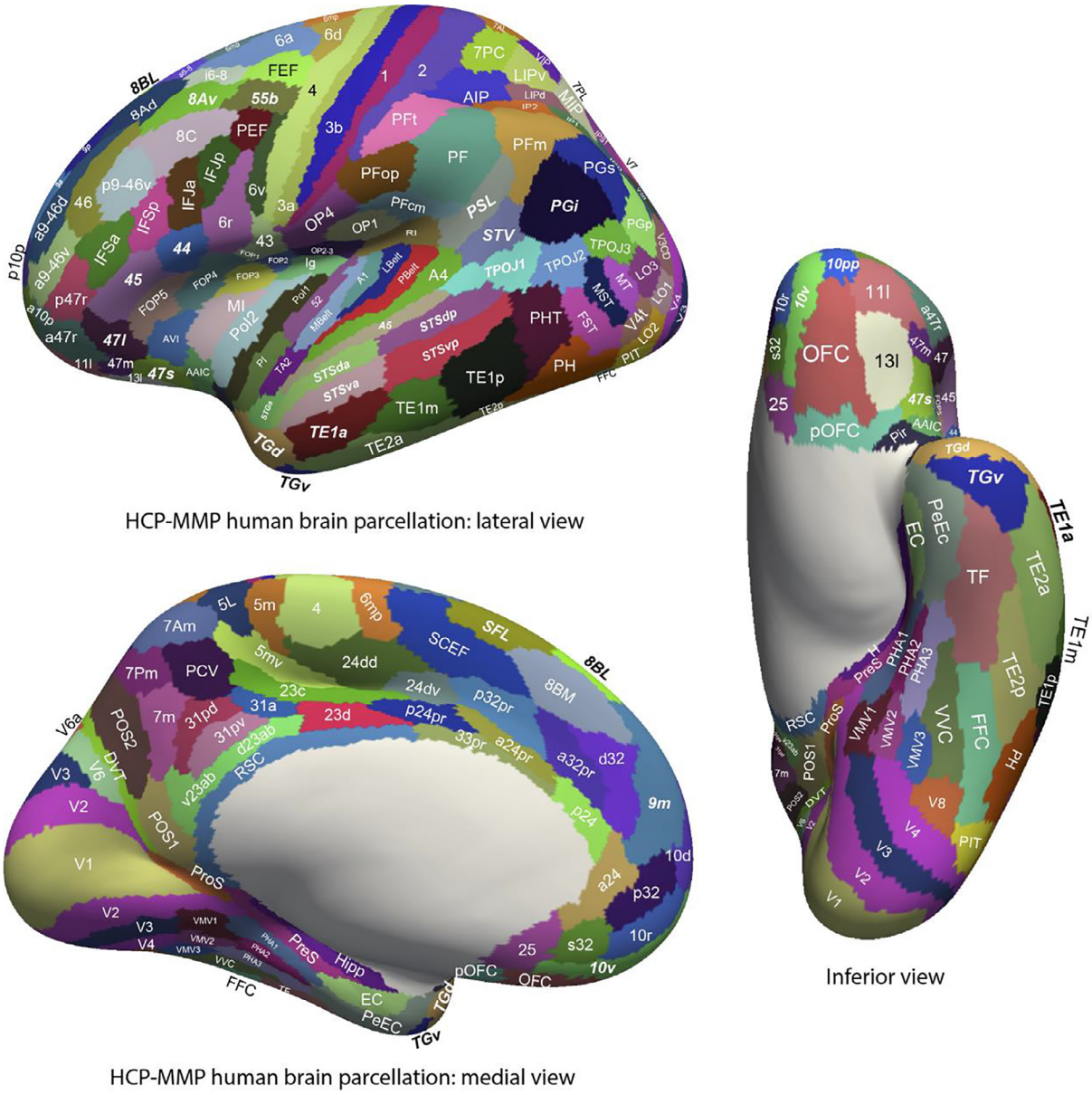

Fig. 1. Language-related regions of interest of the human cortex as defined in the HCP-MMP atlas (Glasser et al., 2016a), and in its extended version HCPex (Huang et al., 2022). The regions are shown on images of the human brain with the sulci expanded sufficiently to allow the regions within the sulci to be shown. The language-related regions identified in the community analysis are shown in bold italic font, and are as follows: Group 1: STSva STSvp TE1a TGd PGi 10v 9m 10pp 47s 8Av 8BL 9a 9p. Group 2: TGv 44 45 47l SFL 55b. Group 3: A5 STGa STSda STSdp PSL STV TPOJ1. Abbreviations are provided in Table S1.

the type widely used in analysis of neuroimaging data (Rubinov and Sporns, 2010). A community analysis was performed on the effective connectivity matrix for all 180 cortical regions in the left hemisphere, using the Brain Connectivity Toolbox (Rubinov and Sporns, 2010) (https://www.nitrc.org/projects/bct). The function modularity_und() was used with gamma=5, and it detected 7 communities of which one contained the following regions: 55b A5 STGa STSda STSdp STSva STSvp TE1a TGd TGv PSL STV TPOJ1 PGi 10v 9m 10pp 47 s 44 45 47l 8Av 8BL9a 9p SFL (for abbreviations see Table S1 and for brain regions see Figs. 1 and S1). As this community contains brain regions implicated in language (including areas 44 and 45 known as Broca's area, the Peri-Sylvian Language area (PSL), and the Superior Frontal Language area (SFL)), this set of 26 regions was selected for the connectivity and diffusion tractography analysis for effective and functional connectivities and connections with all the 360 cortical areas in both hemispheres. A data check showed that exactly the same community of 26 cortical regions was detected if the functional connectivity matrix was used. The community analysis was performed on the left hemisphere as this hemisphere is typically especially involved in language in right-handed people from the population imaged by the HCP, with the right hemisphere involved in for example prosody (Hertrich et al., 2020). 96% of the participants in our sample were right-handed, as shown by their Edinburgh Handedness Inventory scores.

2.4. Measurement of effective connectivity

Effective connectivity measures the effect of one brain region on another, and utilizes differences detected at different times in the signals in each connected pair of brain regions to infer effects of one brain region on another. One such approach is dynamic causal modelling, but it applies most easily to activation studies, and is typically limited to measuring the effective connectivity between just a few brain areas

(Friston, 2009; Valdes-Sosa et al., 2011; Bajaj et al., 2016), though there have been moves to extend it to resting state studies and more brain areas (Razi et al., 2017; Frassle et al., 2017). The method used here (see Rolls et al. 2022b) was developed from a Hopf algorithm to enable measurement of effective connectivity between many brain areas, described by Deco et al. (2019). A principle is that the functional connectivity is measured at time *t* and time *t* + *tau*, where *tau* is typically 2 s to take into account the time within which a change in the BOLD signal can occur, and then the effective connectivity model is trained by error correction until it can generate the functional connectivity matrices at time *t* and time *t* + *tau*. Further details of the algorithm, and the development that enabled it to measure the effective connectivity in each direction, are described next and in more detail in the Supplementary Material.

To infer the effective connectivity, we use a whole-brain model that allows us to simulate the BOLD activity across all brain regions and time. We use the so-called Hopf computational model, which integrates the dynamics of Stuart-Landau oscillators, expressing the activity of each brain region, by the underlying anatomical connectivity (Deco et al., 2017b). As mentioned above, we include in the model 360 cortical brain areas (Huang et al., 2022). The local dynamics of each brain area (node) is given by Stuart-Landau oscillators which expresses the normal form of a supercritical Hopf bifurcation, describing the transition from noisy to oscillatory dynamics (Kuznetsov, 2013). During the last years, numerous studies were able to show how the Hopf whole-brain model successfully simulates empirical electrophysiology (Freyer et al., 2011, 2012), MEG (Deco et al., 2017a) and fMRI (Kringelbach et al., 2015; Deco et al., 2017b; Kringelbach and Deco, 2020).

The Hopf whole-brain model can be expressed mathematically as follows:

$$\frac{dx_i}{dt} = \overbrace{\left[a_i - x_i^2 - y_i^2\right]x_i - \omega_i y_i}^{Local\ Dynamics} + \overbrace{G\sum_{j=1}^{N} C_{ij}\left(x_j - x_i\right)}^{Coupling} + \overbrace{\beta\eta_i(t)}^{Gaussian\ Noise} \quad (1)$$

$$\frac{dy_i}{dt} = \left[a_i - x_i^2 - y_i^2\right]y_i + \omega_i x_i + G\sum_{j=1}^{N} C_{ij}\left(y_j - y_i\right) + \beta\eta_i(t) \quad (2)$$

Eqs. (1) and (2) describe the coupling of Stuart-Landau oscillators through an effective connectivity matrix C. The $x_i(t)$ term represents the simulated BOLD signal data of brain area *i*. The values of $y_i(t)$ are relevant to the dynamics of the system but are not part of the information read out from the system. In these equations, $\eta_i(t)$ provides additive Gaussian noise with standard deviation β. The Stuart-Landau oscillators for each brain area *i* express a Hopf normal form that has a supercritical bifurcation at $a_i = 0$, so that if $a_i > 0$ the system has a stable limit cycle with frequency $f_i = \omega_i/2\pi$ (where ω_i is the angular velocity); and when $a_i < 0$ the system has a stable fixed point representing a low activity noisy state. The intrinsic frequency f_i of each Stuart-Landau oscillator corresponding to a brain area is in the 0.008–0.08 Hz band (i = 1, …, 360). The intrinsic frequencies are fitted from the data, as given by the averaged peak frequency of the narrowband BOLD signals of each brain region. The coupling term representing the input received in node *i* from every other node *j*, is weighted by the corresponding effective connectivity C_{ij}. The coupling is the canonical diffusive coupling, which approximates the simplest (linear) part of a general coupling function. *G* denotes the global coupling weight, scaling equally the total input received in each brain area. While the oscillators are weakly coupled, the periodic orbit of the uncoupled oscillators is preserved. Details are provided in the Supplementary Material.

The effective connectivity matrix is derived by optimizing the conductivity of each existing anatomical connection as specified by the Structural Connectivity matrix (measured with tractography (Huang et al., 2021)) in order to fit the empirical functional connectivity (FC) pairs and the lagged FC^{tau} pairs. By this, we are able to infer a non-symmetric Effective Connectivity matrix (see Gilson et al. 2016). Note that FC^{tau}, ie the lagged functional connectivity between pairs, lagged at *tau* s, breaks the symmetry and thus is fundamental for our purpose. Specifically, we compute the distance between the model FC simulated from the current estimate of the effective connectivity and the empirical data FC^{emp}, as well as the simulated model FC^{tau} and empirical data FC^{tau_emp} and adjust each effective connection (entry in the effective connectivity matrix) separately with a gradient-descent approach. The model is run repeatedly with the updated effective connectivity until the fit converges towards a stable value.

We start with the anatomical connectivity obtained with probabilistic tractography from dMRI (or from an initial zero *C* matrix as described in the Supplementary Material) and use the following procedure to update each entry C_{ij} in the effective connectivity matrix

$$C_{ij} = C_{ij} + \varepsilon\left(FC_{ij}^{emp} - FC_{ij} + FC_{ij}^{tau\_emp} - FC_{ij}^{tau}\right) \quad (3)$$

where ϵ is a learning rate constant, and *i* and *j* are the nodes. When updating each connection if the initial matrix is a dMRI structural connection matrix (see Supplementary Material), the corresponding link to the same brain regions in the opposite hemisphere is also updated, as contralateral connections are not revealed well by dMRI. The convergence of the algorithm is illustrated by Rolls et al. (2022b), and the utility of the algorithm was validated as described below.

For the implementation, we set *tau* to be 2 s, selecting the appropriate number of TRs to achieve this. The maximum effective connectivity was set to a value of 0.2, and was found between V1 and V2.

2.5. Effective connectome

Whole-brain effective connectivity (EC) analysis was performed between the 26 regions described above in the language community and the 360 regions defined in the surface-based HCP-MMP atlas (Glasser et al., 2016a) in their reordered form provided in Table S1 (Huang et al., 2022). This EC was computed for all 171 participants. The effective connectivity algorithm was run until it had reached the maximal value for the correspondence between the simulated and empirical functional connectivity matrices at time *t* and *t* + *tau* (see Supplementary Material).

The effective connectivity calculated between the 360 cortical areas was checked and validated in a number of ways. First, in all cases the 360 × 360 effective connectivity matrix could be used to generate by simulation 360 × 360 functional connectivity matrices for time *t* and time *t* + *tau* that were correlated 0.75 or more with the empirically measured functional connectivity matrices at time *t* and time *t* + *tau* using fMRI. Second, the effective connectivity matrices were robust with respect to the number of participants, in that when the 171 participants were separated into two groups of 86, the correlation between the effective connectivities measured for each group independently was 0.98. Third, the effective connectivities for early visual areas V1, V2, V3, and V4 were compared with the known connections for forward and backward connections involving these areas in macaques (Markov et al., 2014), and the human effective connectivity was consistent with the connections in this hierarchically organised system in macaques, with these results shown in Rolls et al. (2022b). Fourth, the effective connectivity with in particular the corresponding brain region contralaterally was high relative to other contralateral connectivities, providing clear evidence that the effective connectivity algorithm could identify distant brain regions that could be expected to have high effective connectivity.

To test whether the vectors of effective connectivities of each of the 26 language-related cortical regions of interest with the 180 areas in the left hemisphere of the modified HCP atlas were significantly different, the interaction term was calculated for each pair of the 26 effective connectivity vectors in two-way ANOVAs (each 2 × 180) across the 171 participants, and Bonferroni correction for multiple comparisons was applied. This was confirmed with the Scheirer-Rey-Hare non-parametric test.

2.6. Functional connectivity

For comparison with the effective connectivity, the functional connectivity was also measured at 7T with the identical set of participants, data, and filtering of 0.008–0.08 Hz. The functional connectivity was measured by the Pearson correlation between the BOLD signal time-series for each pair of brain regions, and is in fact the FC^{emp} referred to above. A threshold of 0.4 is used for the presentation of the findings in Fig. 5, for this sets the sparseness of what is shown to a level commensurate with the effective connectivity, to facilitate comparison between the functional and the effective connectivity. The functional connectivity can provide evidence that may relate to interactions between brain regions, while providing no evidence about causal direction-specific effects. A high functional connectivity may in this scenario thus reflect strong physiological interactions between areas, and provides a different type of evidence to effective connectivity. The effective connectivity is non-linearly related to the functional connectivity, with effective connectivities being identified (i.e., greater than zero) only for the links with relatively high functional connectivity.

2.7. Connections shown with diffusion tractography

Diffusion tractography can provide evidence about fibre pathways linking different brain regions with a method that is completely different to the ways in which effective and functional connectivity are measured, so is included here to provide complementary and supporting evidence to the effective connectivity. Diffusion tractography shows only direct connections, so comparison with effective connectivity can help to suggest which effective connectivities may be mediated directly or transsynaptically. Diffusion tractography does not provide evidence about the direction of connections. Diffusion tractography was performed on the same 171 HCP participants imaged at 7T with methods described fully elsewhere (Huang et al., 2021) and not repeated here for conciseness, and is shown here for the language cortex areas in Fig. 6. The term 'connections' is used when referring to what is shown with diffusion tractography.

3. Results

3.1. Overview: effective connectivity, functional connectivity, and diffusion tractography

The effective connectivities *to* the language-related regions of interest (ROIs) from other cortical areas in the left hemisphere are shown in Fig. 2. The effective connectivities *from* the ROIs to other cortical areas in the left hemisphere are shown in Fig. 3. The vectors of effective connectivities of each of the 26 ROIs with the 180 areas in the left hemisphere of the HCP-MMP atlas were all significantly different from each other. (The interaction term in a 2-way ANOVA across the 171 participants was $p<10^{-90}$ for the comparisons between every pair of the 26 ROIs regions after Bonferroni correction for multiple comparisons). The functional implications of the results described next are considered in the Discussion.

A community analysis (Rubinov and Sporns, 2010) was performed on the effective connectivities of the 26 language-related ROIs from all 180 cortical areas in the left hemisphere, to investigate whether any grouping could be made. It was found that three communities were formed (gamma=1.2), as follows: Group 1: STSva STSvp TE1a TGd PGi 10v 9m 10pp 47s 8Av 8BL 9a 9p. Group 2: TGv 44 45 47l SFL 55b. Group 3: A5 STGa STSda STSdp PSL STV TPOJ1. The correlations between the effective connectivities of these groups are shown in Fig. S4, and between the functional connectivities in Fig. S5. In the Figures, these groups are sep-

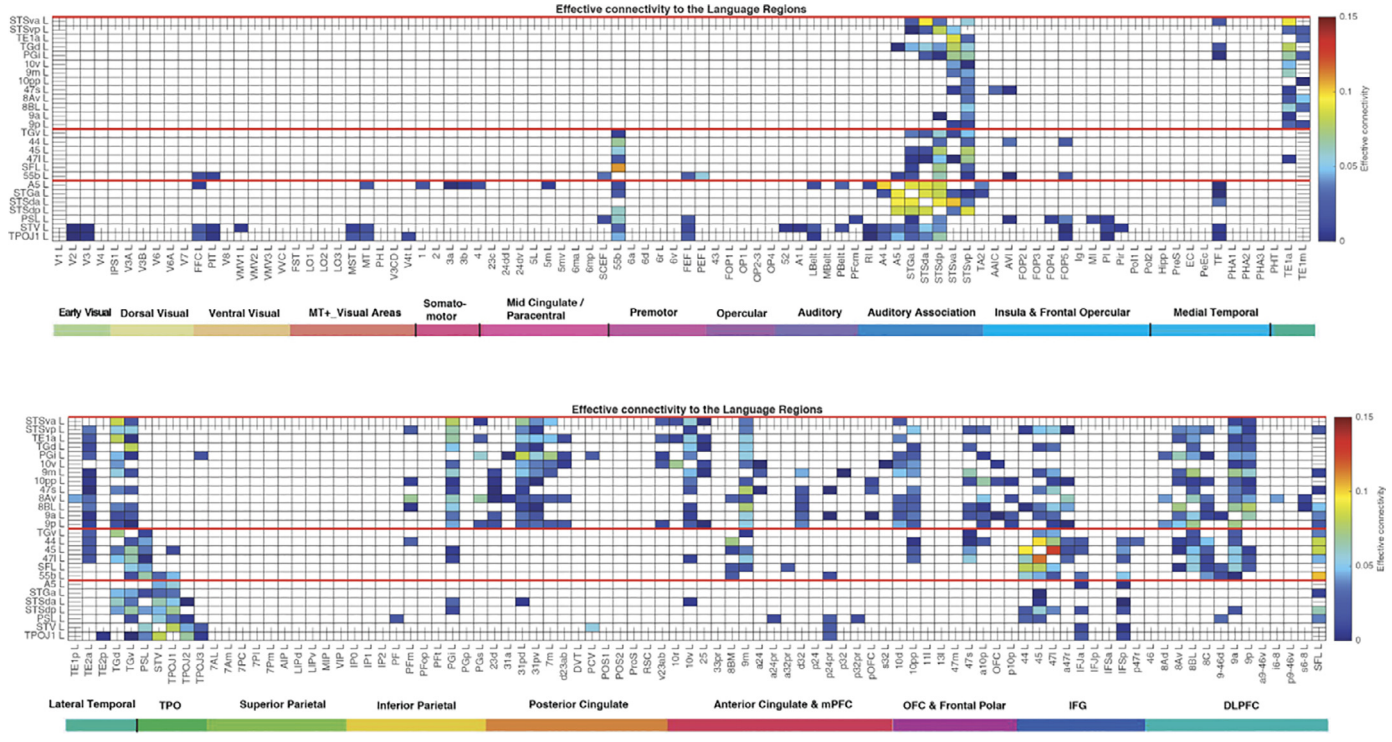

Fig. 2. Effective connectivity *TO* the language-related ROIs (the rows) *FROM* 180 cortical areas (the columns) in the left hemisphere. The effective connectivity is read from column to row. Effective connectivities of 0 are shown as blank. All effective connectivity maps are scaled to show 0.15 as the maximum, as this is the highest effective connectivity found between this set of brain regions. The effective connectivity algorithm for the whole brain is set to have a maximum of 0.2, and this was for connectivity between V1L and V1R. The effective connectivity for the first set of cortical regions is shown in the top panel; and for the second set of regions in the lower panel. Abbreviations: see Table S1. The three groups of language-related ROIs are separated by red lines, with Group 1 at the top, Group 2 in the middle, and Group 3 at the bottom. (ECtoLang.eps) (For interpretation of the references to color in this figure, the reader is referred to the web version of this article.).

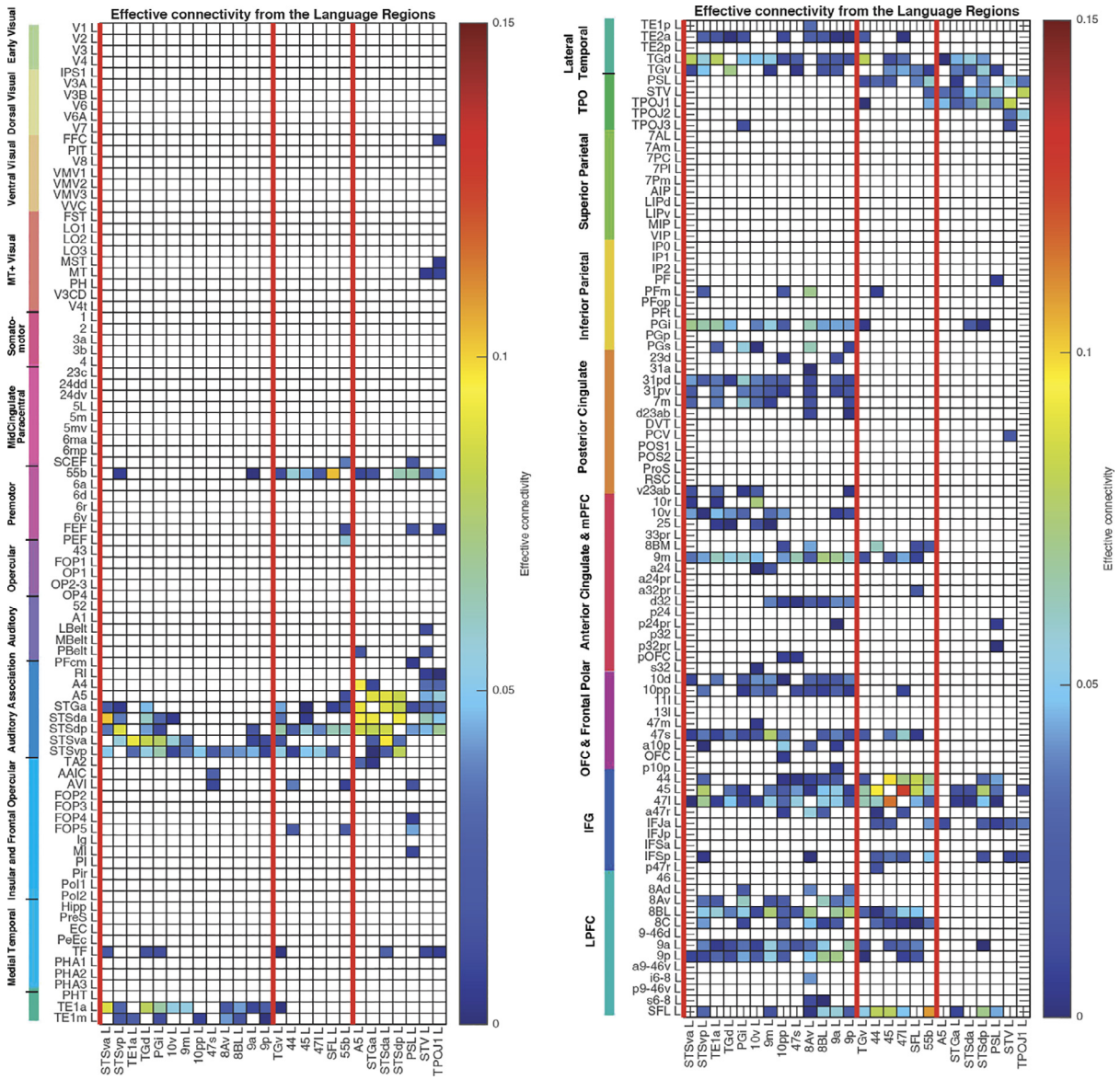

Fig. 3. Effective connectivity *FROM* the language-related ROIs *TO* 180 cortical areas in the left hemisphere. The effective connectivity is read from column to row. Effective connectivities of 0 are shown as blank Abbreviations: see Table S1. The three groups are separated by red lines, with Group 1 on the left, Group 2 in the middle, and Group 3 on the right. (For interpretation of the references to color in this figure, the reader is referred to the web version of this article.).

arated by red lines. It may be helpful to refer to Fig. 7 when considering the Results, for Fig. 7 provides summaries of the effective connectivities of each of the three Groups.

To facilitate the description of the results, each of these groups is considered in turn, taking into account also the difference of the effective connectivities in the two directions for every link (Fig. 4), the functional connectivities (Fig. 5), and the diffusion tractography (Fig. 6). These groups are used to help present the findings, but different HCP-MMP regions within a group do not have identical connectivity, and this shows part of the utility of the HCP-MMP (Glasser et al., 2016a) and the approach taken here. The description starts with the left hemisphere, which is of especial interest as it is more involved in language in right-handed people, but there is a comparison with connectivity in the right hemisphere later. (It is noted that the terms ventral / dorsal are carried over from the names of some brain regions in non-humans, and are equivalent to inferior / superior which could be applied to brain regions in non-human vertebrates. It is also noted that in humans, the greatly developed inferior parietal lobule contains posteriorly PG areas (shown in Fig. 1) found in BA39 in the angular gyrus; and anteriorly contains PF areas found in BA40 in the supramarginal gyrus (Rolls et al., 2022a).)

Group 1. STSva STSvp TE1a TGd PGi 10v 9m 10pp 47s 8Av 8BL 9a 9p.

The topology of this group is interesting, with a whole row of cortical regions extending almost continuously from PGi through the inferior parts of the superior temporal sulcus (STSvp and STSva) and TE1a to reach TGd (Figs. 1 and 7a). Indeed, it is notable that Group 1 includes regions in the inferior parts of the cortex in the superior temporal sulcus (STSva, STSvp, and also the more inferior TE1a), and with the posterior and also relatively inferior parietal region PGi (see Fig. 1). This may thus be thought of as an inferior language-related system as far as the temporal lobe is concerned. It may be helpful to refer to Fig. 7a which provides a summary of the connectivity of a typical Group 1 region.

As shown in Fig. 2, STSvp is one key region, for it has effective connectivity with all Group 1 and 2 regions, and to half of the Group 3 regions. The Group 1 regions receive from *anterior* inferior temporal cortex areas (TE1a, TE1m, TE2a) much more extensively than any

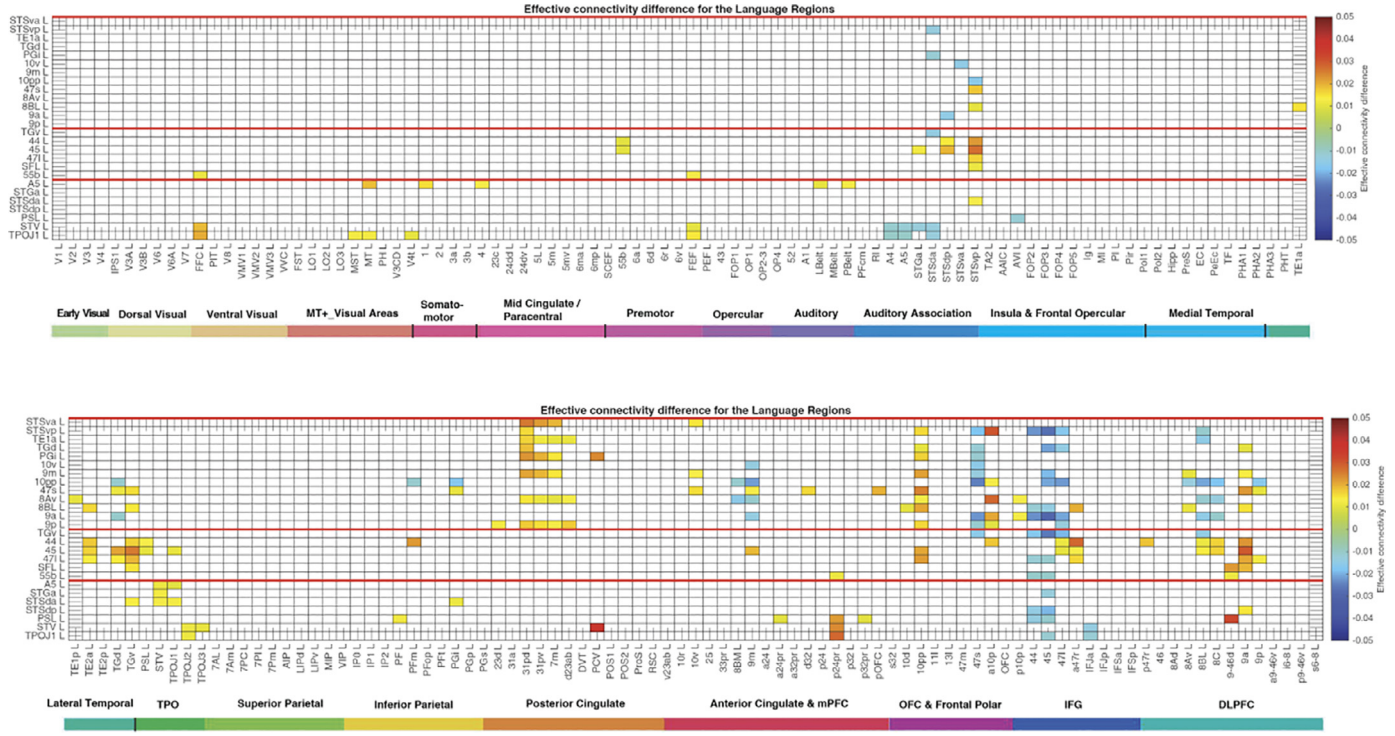

Fig. 4. Difference of the effective connectivity for the language-related ROIs with cortical areas. For a given link, if the effective connectivity difference is positive, the connectivity is stronger in the direction from column to row. For a given link, if the effective connectivity difference is negative, the connectivity is weaker in the direction from column to row. This is calculated from 171 participants in the HCP imaged at 7T. The threshold value for any effective connectivity difference to be shown is 0.01. The abbreviations for the brain regions are shown in Table S1, and the brain regions are shown in Figs. 1 and S1. The effective connectivity difference for the first set of cortical regions is shown in the top panel; and for the second set of regions in the lower panel.

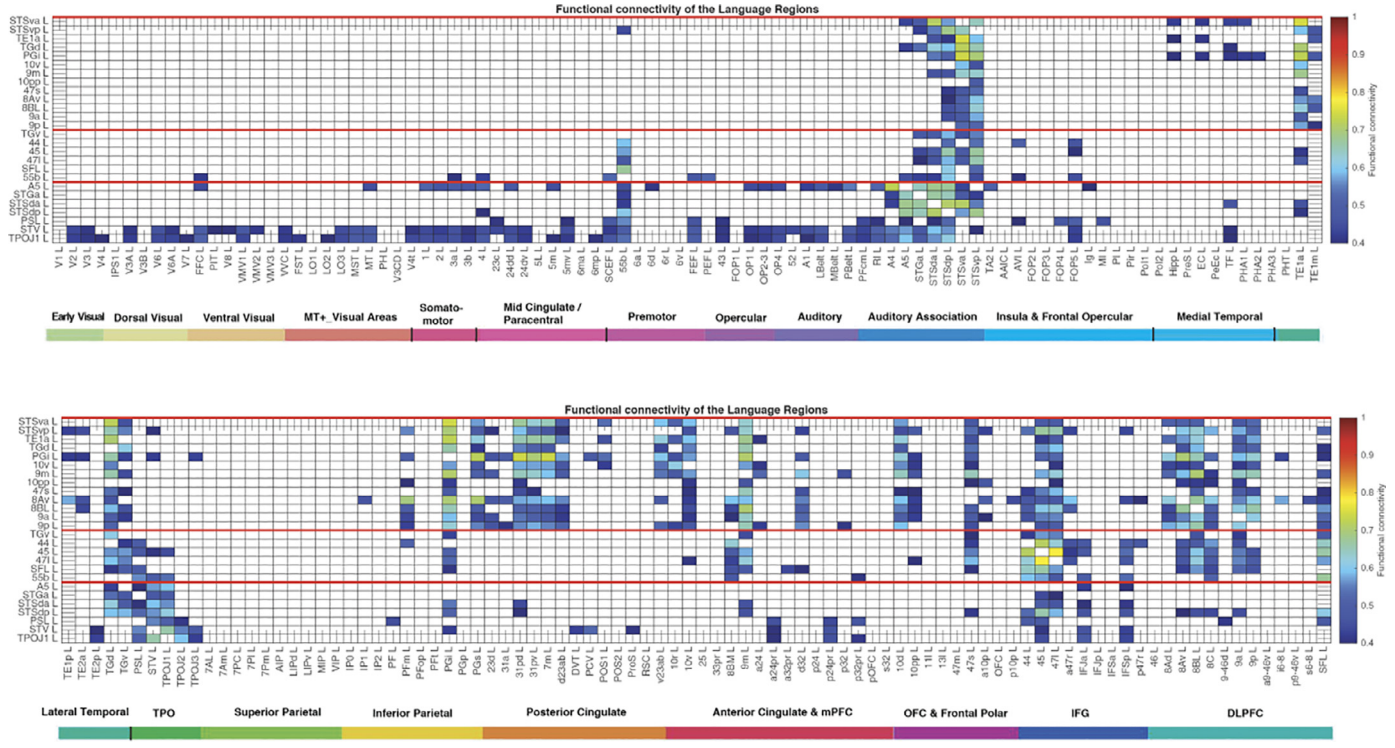

Fig. 5. Functional connectivity between the language-related ROIs and 180 cortical areas in the left hemisphere. Functional connectivities less than 0.4 are shown as blank. The upper figure shows the functional connectivity of the 26 language-related ROIs with the first half of the cortical areas; the lower figure shows the functional connectivity with the second half of the cortical areas. Abbreviations: see Table S1. The three groups of language-related areas are separated by red lines, with Group 1 at the top. (For interpretation of the references to color in this figure, the reader is referred to the web version of this article.).

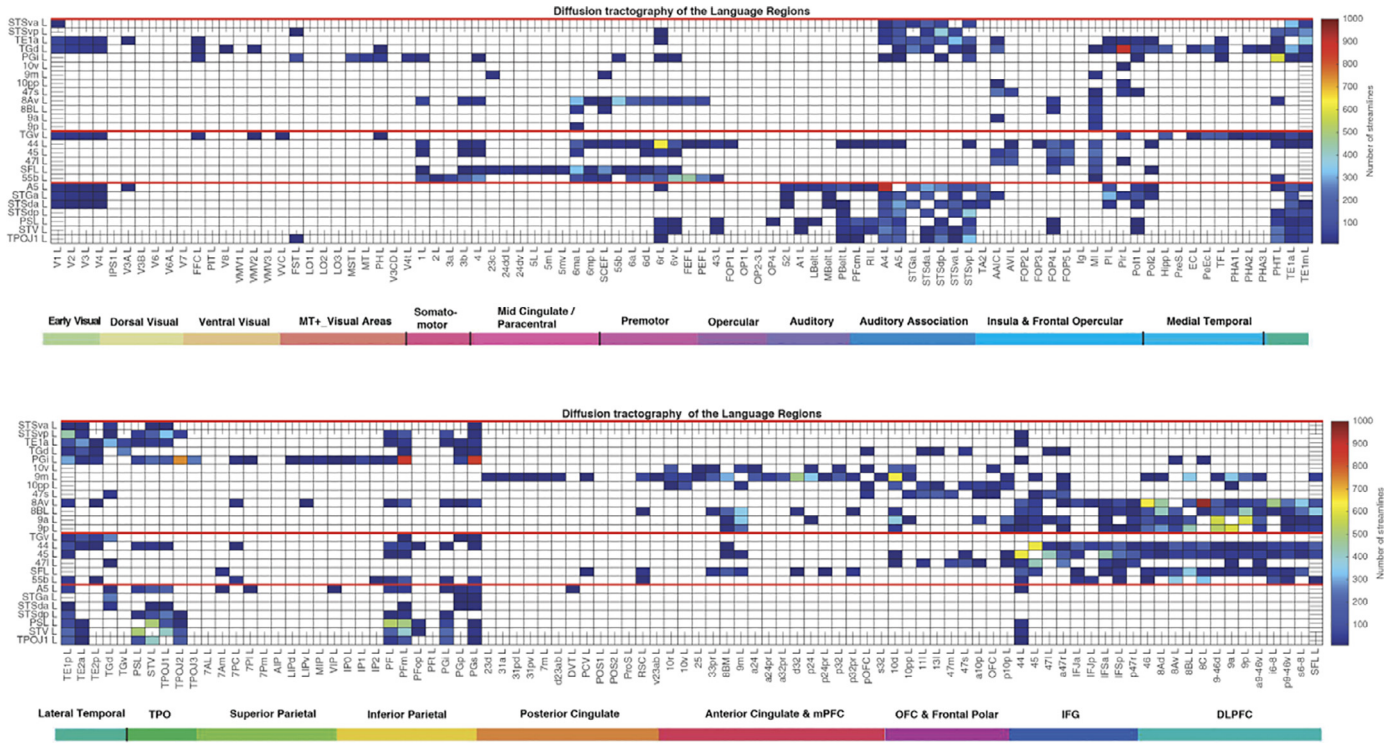

Fig. 6. Connections between the language-related ROIs and 180 cortical areas in the left hemisphere as shown by diffusion tractography using the same layout as in Figs. 2 and 5. The number of streamlines shown was thresholded at 10 and values less than this are shown as blank. Abbreviations: see Table S1. The three groups are separated by red lines, with Group 1 at the top. (For interpretation of the references to color in this figure, the reader is referred to the web version of this article.).

other Group. In common with other groups, the Group 1 regions have effective connectivity with the temporal pole (TGd, TGv). The Group 1 regions also have connectivity with parietal areas (especially PGi, and to some extent PF and PGs) much more extensively than other groups. Further, the Group 1 regions are also different from the other Groups in having substantial effective connectivity with the posterior cingulate cortex, especially with the posteroventral parts 31pv, 31pd, 7m, d23ab and v23ab that are implicated in episodic memory (Rolls et al., 2022d); and these regions also have connectivity with TF which is the ventral stream part of the parahippocampal gyrus (Rolls et al., 2022b). Group 1 also has effective connectivity with the medial orbitofrontal cortex (OFC and pOFC) and related ventromedial prefrontal cortex areas 9m, d32, 10v and 10r (Rolls et al., 2022c); and with the frontal pole p10p, 10pp and 10d. Group 1 also has effective connectivity with region 45 (part of Broca's area); and the adjacent regions 47s and 47l (which appear to be parts of the inferior frontal gyrus / lateral orbitofrontal cortex that at least in the left hemisphere are closely related to language). Group 1 has extensive effective connectivity with dorsolateral prefrontal cortex regions (as does Group 2 but not Group 3), including areas 8Av, 8BL, 8C, 9a and 9p. There is also some effective connectivity with the Superior Frontal Language area (SFL). Group 1 (in contrast with Groups 2 and 3) has no effective connectivity with IFJa and IFSp (which are just superior to region 44). Group 1 receives no effective connectivity from the Peri-Sylvian Language area (PSL), the Superior Temporal Visual area (SVT), or the temporal-parietal-occipital junction (TPOJ) regions.

Figs. 3 and 4 show that the effective connectivities are directed more strongly towards than away from Group 1 regions for the inferior temporal cortex and temporal pole regions, for the posterior cingulate cortex, and for the frontal pole. (These regions thus connect to Group 1 regions.) Conversely, the effective connectivities are stronger from these Group 1 areas to areas 44, 45 and 47s, which can be seen as output regions for the Group 1 regions.

Fig. 5 shows that the functional connectivities are generally consistent, but shows in addition some interactions of Group 1 regions with the hippocampus and entorhinal cortex (as well as with TF); and some more interaction with region 44 in addition to 45 (Broca's area).

Fig. 6 provides an indication of no direct connections between STS regions and Group 1 regions 10v 9m 10pp 47s 8Av 8BL 9a 9p, so these effective connectivities may reflect indirect effects. Similarly, the tractography did not reveal connections between the temporal lobe regions of Group 1 and prefrontal cortical areas, so these may be indirect effects. There is also some indication from the tractography for further connections between some sensory systems (e.g., somatosensory regions 1-3 and the insula) and Group 1 regions.

In summary, the Group 1 regions form a community that receives from a number of brain areas close to the top of processing hierarchies; has connectivity with reward value / emotion-related medial orbitofrontal cortex and related ventromedial prefrontal cortex areas; with hippocampal system memory-related regions; and with the frontal pole; and has effective connectivity directed to a number of Group 2 areas, including regions 44 and 45 that relate to Broca's area. These Group 1 regions tend to relate to inferior STS regions (STSva and STSvp).

Group 2. TGv 44 45 47l SFL 55b.

Group 2 includes mainly frontal lobe regions, but includes TGv. It may be helpful to refer to Fig. 7c which provides a summary of the connectivity of a typical Group 2 region.

As shown in Fig. 2, the Group 2 regions have robust effective connectivity with 55b (located in premotor cortex between the frontal eye fields FEF and PEF); with superior (STSda, STSdp, STGa) as well as an inferior region (STSvp but much less STSva) in the superior temporal sulcus (STS); TE2a; the Peri-Sylvian Language area (PSL) (and some connectivity with nearby STV and TPOJ1); medial prefrontal 8BM and 9a; some connectivity with the frontal pole (10pp, a10p); strong effective connectivity between the members of this group such as 44, 45, 47l but also with the nearby a47r and 47s; with inferior frontal gyrus IFja and IFSp; with dorsolateral prefrontal cortex regions; and especially strongly with the Superior Frontal Language area (SFL). A difference between the effective connectivity of 44 and 45 is that 45 receives effective

connectivity from more Group 1 regions, including TGd, 9m, 9a, 8Av and 47 s.

Fig. 4 (together with Figs. 2 and 3) shows that most of these effective connectivities are directed more towards than away from the Group 2 regions, with the blue colours for regions 44 and 45 showing that these are recipient regions from all of these cortical regions, including the other parts of Group 2, namely TGv, 47l, SFL, and 55b. However, Fig. 3 makes it clear that regions to which regions 44 and 45 do connect towards include premotor 55b; STSdp and STSvp; medial prefrontal 8BM and 9m; 47l, IFJa and IFSp; 8BL and 8C; and especially strongly to the Superior Frontal Language area (SFL). SFL and 55b are likely to be especially important outputs of areas 44 and 45, given the premotor locations of 55b and SFL in the brain.

Group 2 differs from Group 1 in having strong effective connectivity with 55b; in including more connectivity with superior STS areas (STSda, STSdp and also STGa) and less with STSva an inferior STS region; in having little connectivity with TE1a and TE1m though there is connectivity with TE2a; in having connectivity with inferior frontal gyrus regions IFja and IFSp (which are just superior to 44 and 45); and in having especially strong effective connectivity with SFL.

The functional connectivity (Fig. 5) is consistent, and the diffusion tractography (Fig. 6) is also consistent, but provides also an indication

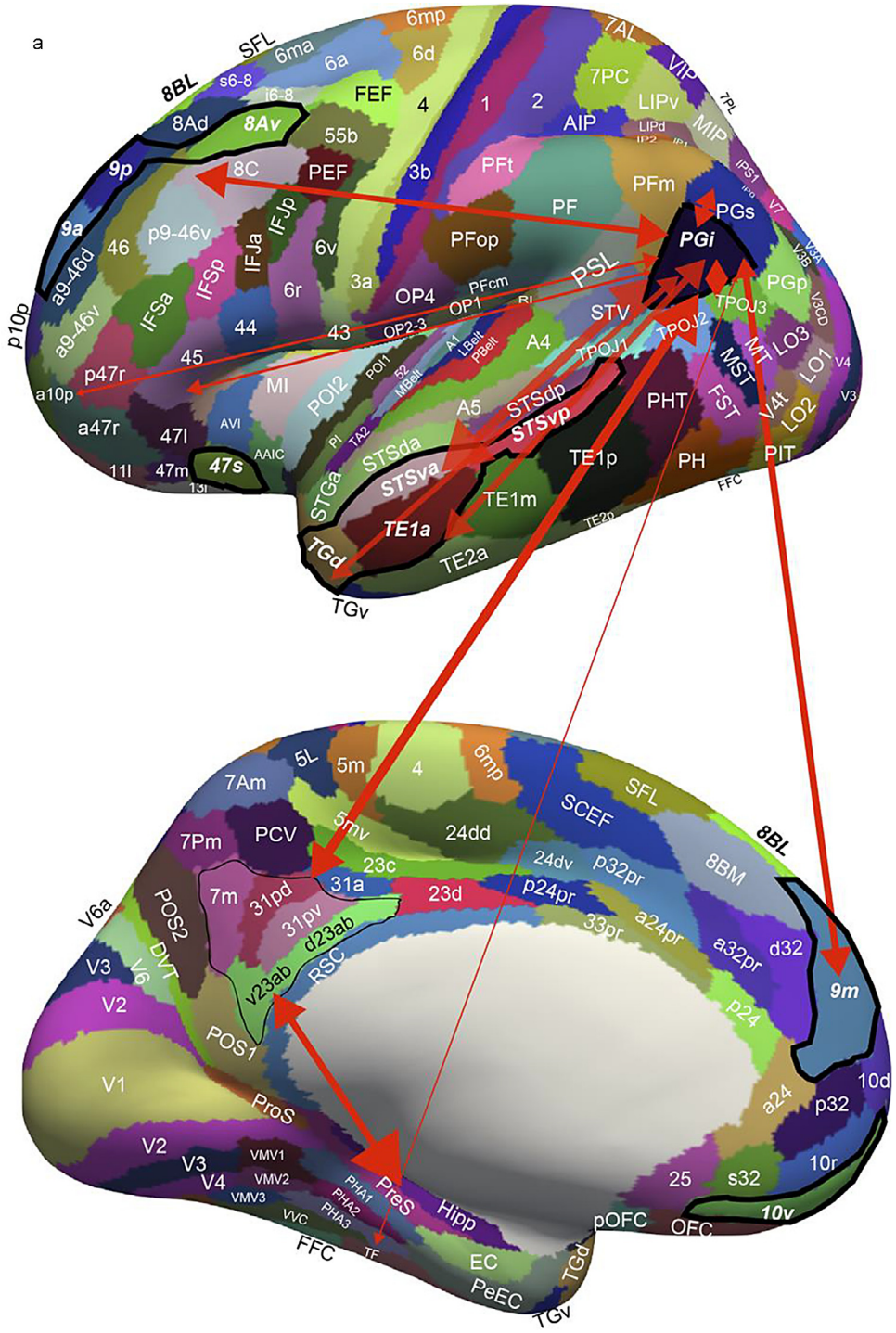

Fig. 7. a. Effective connectivity of region PGi chosen as an example of a Group 1 region with connectivity with the inferior STS stream, the posterior cingulate cortex, the frontal pole, and the dorsolateral prefrontal cortex. The Group 1 regions are indicated in bold italic font and are outlined in black (including PGi), and are: STSva STSvp TE1a TGd PGi 10v 9m 10pp 47s 8Av 8BL 9a 9p. The widths of the lines and the size of the arrowheads indicate the magnitude and direction of the effective connectivity, which are shown in Table S2. 7PM and IP1 connect to PGs which in turn connects to PGi, providing a route for PGi to receive visual motion information, and to connect that to areas such as STSva and STSvp. The thin black outline encloses the postero-ventral memory-related regions of the posterior cingulate cortex, which connect to the hippocampal system (Rolls et al., 2022d). (ParBrainSummaryPGiLang2.eps) b. Effective connectivity of region TPOJ1 chosen as an example of the typical effective connectivity of a Group 3 region with connectivity with a superior STS auditory-visual stream extending from STGA through STSda, A5, STSdp to TPOJ1. The Group 3 regions are indicated in bold italic font and are outlined in black, and are: A5 STGa STSda STSdp PSL STV TPOJ1. TPOJ1 also has effective connectivity with PSL, STV, TPOJ2, the inferior frontal gyrus IFJA and IFSp and 45, and with premotor area 55b and the midcingulate cortex p24pr. There is also effective connectivity with parahippocampal TF. The widths of the lines and the size of the arrowheads indicate the magnitude and direction of the effective connectivity. c. Effective connectivity of region 45 chosen as an example of the effective connectivity of a Group 2 region. The Group 2 regions are indicated in bold italic font and are outlined in black, and are: TGv 44 45 47l SFL 55b. There is connectivity with the superior STS auditory-visual stream (e.g., STSdp and STGa), with the inferior STS visual stream (e.g., STSvp and TG), with the Peri Sylvian Language area and TPOJ1, with nearby inferior frontal gyrus regions 44, IFSp, 47l and 47s. Probable output regions for 45 include premotor 55b and the (supplementary area) Superior Frontal Language region (SFL). There is some effective connectivity too with the frontal pole, dorsolateral prefrontal 9a and 8BL. The widths of the lines and the size of the arrowheads indicate the magnitude and direction of the effective connectivity.

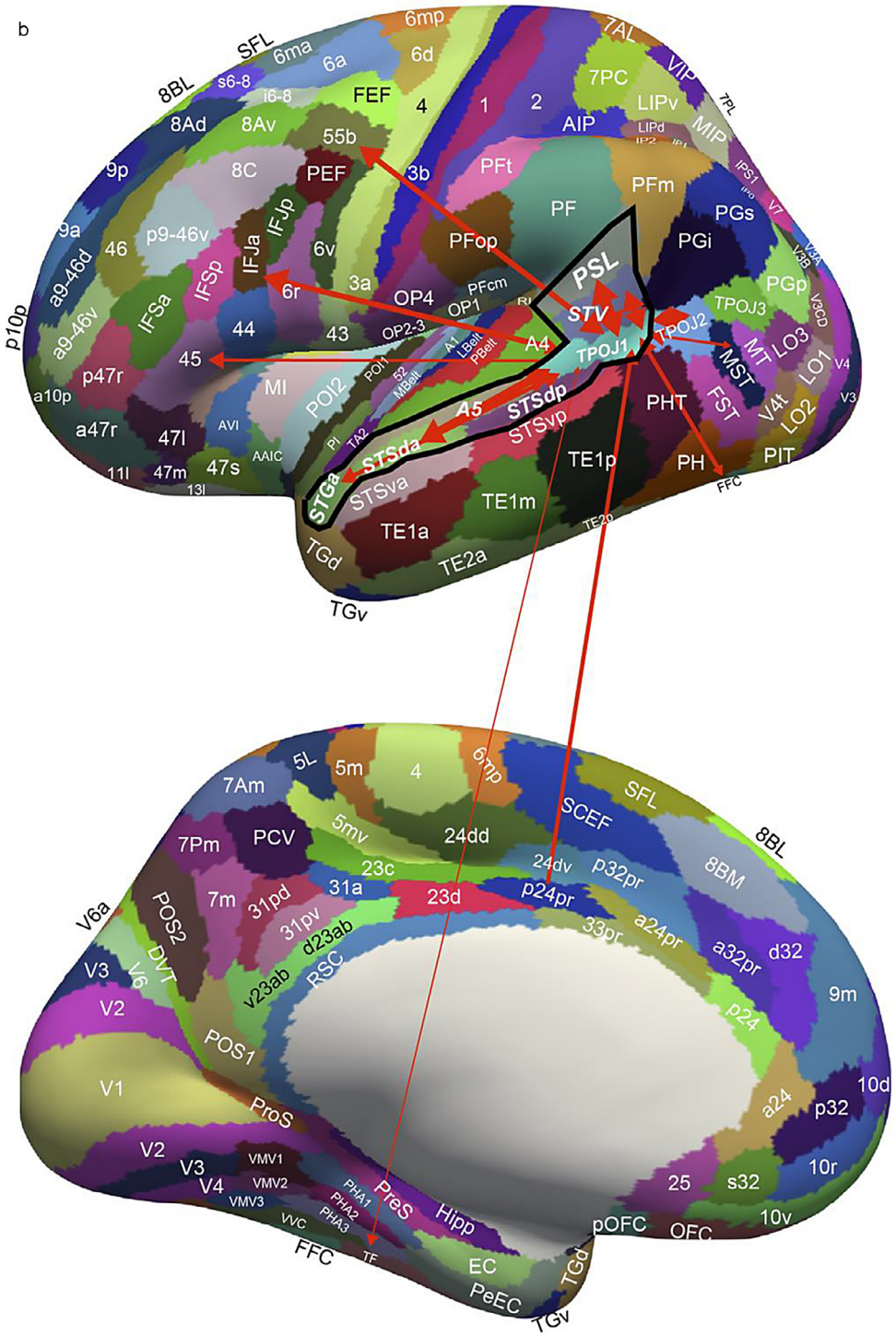

Fig. 7. Continued

that some Group 2 regions have connections with some early sensory cortical regions (visual, somatosensory, auditory, and olfactory (Pir)).

Group 3. A5 STGa STSda STSdp PSL STV TPOJ1

It is notable that Group 3 includes regions in the superior parts of the cortex in the superior temporal sulcus (STSda, STSdp, and also the more superior STGa), and with the posterior and also relatively superior continuous set of regions A5, TPOJ1, STV, and PSL (see Figs. 1 and 7b). This may thus be thought of as a superior language-related system as far as the temporal lobe is concerned. It may be helpful to refer to Fig. 7b which provides a summary of the connectivity of a typical Group 3 region.

Overall, the Group 3 regions have effective connectivity with 55b; with parahippocampal TF; with temporal pole TGv and TGd; with 44 and 45; with inferior prefrontal IFJa and IFsp; some connectivity with the Superior Frontal Language region (SFL); and rather little connectivity with dorsolateral prefrontal cortex (Fig. 2). In addition, the TPOJ1 and STV regions have effective connectivity with some visual cortical regions (FFC, PIT, MST, MT, FEF); some auditory regions (Belt regions, A1, A4, A5, which are immediately superior to the STSdp regions; somatosensory regions in the frontal operculum (FOP, insula and parietal PF); TPOJ2 and TPOJ3; p24pr in the midcingulate premotor cortex (Rolls et al., 2022d) (which with a24pr and p32pr also receives from the

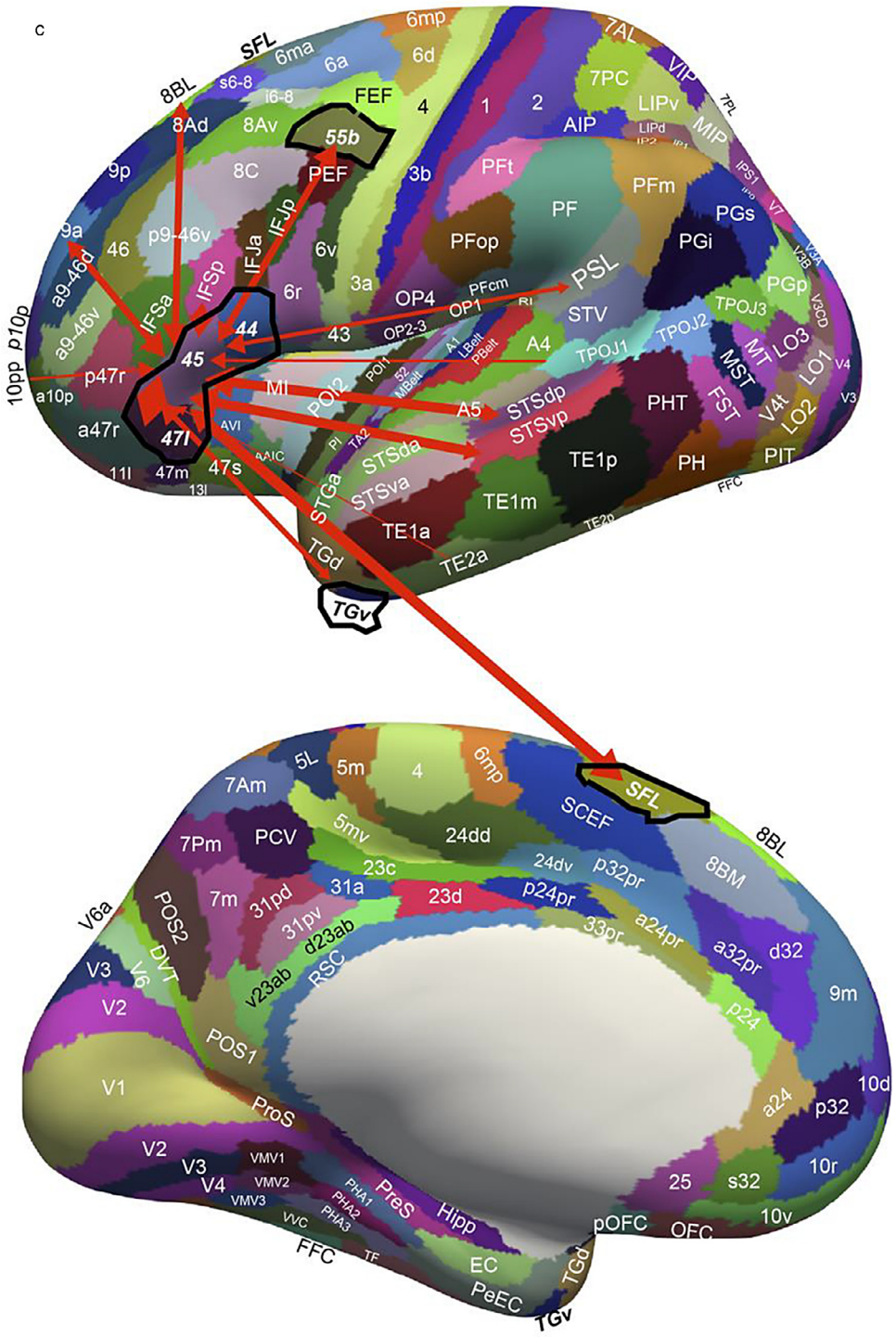

Fig. 7. Continued

PeriSylvian Language region PSL, suggesting the midcingulate cortex as an output region for the PSL). The functional connectivity (Fig. 5) emphasises connectivity with a number of somatosensory cortical regions.

Fig. 4 (and Figs. 3 and 2) show that the effective connectivities just described are stronger towards the Group 3 regions, except that the Group 3 regions (as does Group 1) have stronger effective connectivity directed towards regions 44 and 45 (related to Broca's area).

3.2. *Effective connectivities of the language-related ROIs with contralateral cortical regions*

The effective connectivities of the language-related ROIs from contralateral cortical areas are shown in Fig. S2, and to contralateral cortical areas in Fig. S3. The contralateral effective connectivities are in general weaker than those ipsilaterally. (The ratio across the matrices shown in Figs. 2 and S2 was that the contralateral effective connectivities were 24% of the ipsilateral effective connectivities.).

3.3. *Differences of effective connectivities of the right vs left hemisphere for the language-related regions in the left hemisphere*

Most of the analysis presented so far has been for the left hemisphere, or of the left hemisphere with the right hemisphere. For completeness, the differences of effective connectivity for the Right *minus* the Left hemisphere for the language-related ROIs are shown in Figs. S6 and S7. The blue colour in Figs. S6 and S7 indicates stronger effective

connectivity in the left hemisphere, and is found for many of the STS and related auditory cortex regions; to 55b which is proposed as a premotor output region for vocalization; the temporal pole regions TGv and TGd; parietal PGi; the frontal pole regions (10 and 9); inferior frontal regions 44, 45, 47l and IFSp; and for dorsolateral prefrontal 8Av.

4. Discussion

The results reveal the following connectional principles of language systems in the human brain, summarized for Groups 1–3 in Fig. 7.

(1) A system (Group 1) involving cortical inferior regions of the superior temporal sulcus (STS) with the adjacent inferior temporal visual cortex TE1a and temporal pole TG and the connected parietal PGi regions has effective connectivity with inferior temporal visual cortex (TE) regions, with parietal PFm which also has connectivity with visual regions, with posterior cingulate cortex and parahippocampal TF memory-related regions, with the frontal pole, with the medial orbitofrontal cortex and related ventromedial prefrontal cortex reward-related regions, with the frontal pole, with the dorsolateral prefrontal cortex, and with 44 and 45 ('Broca's area') for output regions. It also receives inputs from PGs which includes visuo-motor as well as visual object system connectivity (Rolls et al., 2022a). It is proposed later in the Discussion that this system can build in its temporal lobe (inferior STS and TG) and parietal parts (PGi and PGs) semantic representations of objects incorporating especially their visual properties. Damage to parts of this system may be associated with for example alexia.

(2) Another system (Group 3) involving superior regions of the superior temporal sulcus (STS) and a whole set of superior temporal lobe regions (including STGa, auditory A5, TPOJ1, the STV and the Peri-Sylvian Language area (PSL)) have effective connectivity with auditory areas (A1, A4, A5, Pbelt), with relatively early visual areas involved in motion, e.g., MT and MST, and faces (FFC), with somatosensory regions (frontal opercular FOP, insula and parietal PF), with other TPOJ regions, and with the inferior frontal gyrus regions (IFJa and IFSp). It is proposed later in the Discussion that this system builds semantic representations specialising in auditory and the related facial motion information useful in theory of mind and somatosensory / body image information, with outputs directed not only to regions 44 and 45, but also to premotor 55b and midcingulate premotor cortex. Damage to parts of this system might be associated with for example problems in auditory comprehension and phonology. Both Groups 1 and 3 have access to the hippocampal episodic memory system via parahippocampal TF.

(3) A largely frontal system (Group 2: regions 44, 45, 47l; 55b; and the Superior Frontal Language region (SFL)) especially associated with the temporal pole TGv, appears to provide output regions for the other parts of the language system, and is likely it is suggested below to be involved in speech production and syntax.

The functions of the different groups of language-related regions are now considered in the light of their connectivity, and the functions of the cortical areas with which they are connected.

Group 1. STSva STSvp TE1a TGd PGi 10v 9m 10pp 47s 8Av 8BL 9a 9p.

The Group 1 network includes inferior (ventral) regions of the cortex in the Superior Temporal Sulcus (STSva and STSvp). The many different high-level cortical areas with which the Group 1 regions (inferior in the temporal lobe and with connectivity with the dorsolateral prefrontal cortex, see Fig. 7a) have connectivity indicates their roles in multimodal especially visual and value-related semantic representations.

The connectivity with inferior temporal cortex TE areas provides for transform-invariant visual representations of objects and faces as shown by discoveries in macaques (Perrett et al., 1982; Booth and Rolls, 1998; Lehky and Tanaka, 2016; Freiwald, 2020; Rolls, 2021c, 2021a; Arcaro and Livingstone, 2021) with complementary evidence from human neuroimaging (Kanwisher et al., 1997; Collins and Olson, 2014; Finzi et al., 2021). The connectivity with inferior parietal cortex PGi and to a smaller extent PGs regions may allow information about the visual motion of objects, such as a head turning away, or the eyes closing, or the lips moving, to convey a social signal such as a greeting (lip-smack) or threat, or when vocalizing, to reach STS areas (Rolls et al., 2022a). Indeed, it was discovered that single neurons in the macaque STS respond to face expression and also to face and head movement to encode the social relevance of stimuli (Hasselmo et al., 1989b, 1989a). For example, a neuron might respond to closing of the eyes, or to turning of the head away from facing the viewer, both of which break social contact (Hasselmo et al., 1989b,1989a). Some neurons respond to the direction of gaze (Perrett et al., 1987). It was found that many of the neurons in the STS respond only or much better to moving faces or objects (Hasselmo et al., 1989a), whereas in the anterior inferior temporal cortex neurons were discovered that respond well to static visual stimuli, and are tuned for face identity (Perrett et al., 1982; Rolls, 1984; Hasselmo et al., 1989a; Rolls et al., 1997b, 1997a; Rolls, 2000; Rolls and Treves, 2011). It has been proposed that PGi, with its inputs from PGs which has connectivity with superior parietal and intraparietal regions that encode visual motion, is part of this processing stream for socially relevant face-related information (Rolls et al., 2022a). Consistent with this, the effective connectivity is stronger from PGi to STS regions (Figs. 2–4). In humans, representations of this type could provide part of the basis for the development of systems to interpret the significance of such stimuli, including theory of mind. Consistent with this proposal, activations in the temporo-parietal junction region are related to theory of mind (Schurz et al., 2017; Buckner and DiNicola, 2019; DiNicola et al., 2020). Signals of this type are important in understanding the meaning of seen faces and objects, and indeed evidence about moving objects present in the STS may reach it from PGs and PGi, which in turn receive connectivity from the intraparietal sulcus regions (Rolls et al., 2022a) in which neurons respond to visual motion and to grasping objects which are important in tool use (Maravita and Romano, 2018), which is another fundamental aspect of the meaning or semantics of stimuli.

Effective connectivity of the Group 1 regions with the frontal pole (10pp, 9m, 9a, 9p) regions implicated in planning and sequencing (Shallice and Burgess, 1996; Gilbert and Burgess, 2008; Shallice and Cipolotti, 2018) and prospective as well as retrospective memory (Underwood et al., 2015) is likely to provide information about the temporal order / sequence of events, which is important in interpreting causal interactions in the world (Rolls, 2021d).

Similarly, the connectivity via the parahippocampal TF region (Figs. 2 and 3) with the hippocampal system implicated in episodic memory (Dere et al., 2008; Moscovitch et al., 2016; Rolls, 2018; Ekstrom and Ranganath, 2018; Rolls, 2021a) is likely to be important in building semantic information about the semantic meaning of events by enabling the memory of particular past events to be taken into account. The connectivity of the Group 1 regions with the postero-ventral parts of the posterior cingulate cortex which are implicated in episodic memory (Vann et al., 2009; Leech and Sharp, 2014; Leech and Smallwood, 2019; Rolls et al., 2022d) by providing a route to the hippocampal system may in a similar way be important in enabling the Group 1 regions, especially those in the temporal lobe but also in the inferior parietal cortex (Papagno, 2018; Davis et al., 2018), to build semantic representations by taking particular previous episodes into account. Consistent with this, increasing activation of the angular gyrus and decreasing activation of the hippocampus occurs when episodic memories become incorporated into schemas (van der Linden et al., 2017).

The connectivity of the Group 1 regions with the orbitofrontal cortex (OFC and pOFC, Fig. 2), pregenual anterior cingulate cortex (d32, Fig. 2) and some ventromedial prefrontal cortex regions where re-

ward value and emotion are represented (Grabenhorst and Rolls, 2011; Cai and Padoa-Schioppa, 2012; Rolls, 2014; Reber et al., 2017; Padoa-Schioppa and Conen, 2017; Rolls, 2019b, 2019a; Rolls et al., 2020b; Rolls, 2021b; Rolls et al., 2022c) provides another fundamental type of input for building semantic representations about people and objects.

The extensive connectivity of the Group 1 regions with the dorsolateral prefrontal cortex (Fig. 2) which is implicated in working memory and planning (Goldman-Rakic, 1996; Baddeley, 2021) is likely to enable semantic representations to be held online to facilitate planning, reasoning, and rearrangement of the order of components if a task fails (Rolls, 2020).

Group 3. A5 STGa STSda STSdp PSL STV TPOJ1

The Group 3 network includes superior (or dorsal) parts of the cortex in the Superior Temporal Sulcus (STSda and STSdp) in the temporal lobe that have auditory as well as early visual inputs, continues up through the temporo-parietal junction (TPOJ1) into the Superior Temporal Visual region (STV) to the Peri Sylvian Language area (PSL), and connects with inferior frontal gyrus areas IFSp and IFJp (rather than dorsolateral prefrontal cortex) and with areas 44 and 45 (related to Broca's area) (Figs. 1 and 7b). Region A5 is adjacent to STSdp (Fig. S1).

There is robust effective connectivity with auditory association cortex, including A5, A4 and to some extent LBelt, PBelt and TA2 (Figs. 2 and 3). The visual input is not from inferior temporal visual cortex (TE regions), but instead with some earlier visual cortical regions involved in motion processing (MST, MT, especially to STV and TPOJ1) and in face processing (the fusiform face cortex FFC and posterior inferior temporal cortex PIT). These inputs are likely to contribute to the neurons discovered in the STS that respond to biological motion such as moving parts of faces such as the lips and eyelids and to the head turning towards vs away from the viewer in object-based coordinates, and also to face expression (Hasselmo et al., 1989b, 1989a). Activations to corresponding stimuli are found in similar posterior STS regions in humans (Critchley et al., 2000; Bellot et al., 2021). It was proposed that this STS region is a third visual system that combines inputs from dorsal and ventral visual streams (Baylis et al., 1987; Hasselmo et al., 1989b, 1989a), and this has recently received support (Pitcher and Ungerleider, 2021). Moreover, the same STS regions also contain neurons that respond to auditory stimuli including in some cases vocalization (Baylis et al., 1987). It is likely that neurons in these STS regions respond to combinations of auditory and synchronized visual stimuli such as vocalization and moving lips and are important in speech analysis by the viewer/hearer not only in noisy environments, but also to confirm who is speaking, and to learn associations between the sight of a person's face and the sound of their voice, which is part of what is required for the semantic representation of a person. Neurons of these types, including face expression, underlie the importance of this region in interpreting the social meaning of visual and auditory stimuli, which is a key part of semantic representations implemented in these STS regions, and that contribute to theory of mind, that is, of another individual's intentions and even thoughts.

Another type of influence on these Group 3 regions comes from somatosensory cortical areas, as is especially evident in the functional connectivity (Fig. 5). The functional connectivity is not only with 1-3b and 5, but also with frontal opercular and insular cortex, and there is some evidence for this too in the effective connectivity, including with parietal PF which can be considered as the top of the somatosensory hierarchy (Rolls et al., 2022a) (Figs. 2 and 3). This may contribute to semantic representations of body image and the sense of self (Rolls et al., 2022a).

The effective connectivity of these Group 3 regions with the inferior frontal gyrus regions and with areas 44 and 45 is proposed to provide inputs to a set of attractor networks in these IFG regions (Rolls and Deco, 2015), supported by the large number of recurrent collaterals onto each neuron in the inferior frontal gyrus (Elston et al., 2006; Elston, 2007), that are important in some particularly temporal aspects of speech production. Indeed, it is proposed that a set of attractor networks in these inferior frontal gyrus regions are linked by stronger forward than backwards connections, and so naturally implement a temporal trajectory or sequence through the series of attractors that implements by learning the sequential constraints that are a key part of syntax in languages in which word order is important in syntax (Rolls and Deco, 2015). According to this theory of speech / language production, the biases for the content of what is in each attractor, e.g., the subject attractor=Jane, the verb attractor=jumps over, and the object attractor=John, come from the temporal lobe semantic regions being considered here, and the execution of the learned syntax comes from the temporally linked series of attractors for the parts of a sentence in the inferior frontal gyrus / Broca's area (Rolls and Deco, 2015). The large extent of the inferior frontal gyrus with effective connectivity in humans (IFSp and IFJa, 44 and 45, 47l and 47s) with these temporal lobe semantic regions including TG is consistent with many sequential syntax-related order-dependent attractor networks in these inferior frontal regions, as it is likely that different attractor systems are required for the active vs passive voice and for different languages in which the word order is different (Rolls and Deco, 2015).

The functions of each of these brain regions is a topic of great interest that is being facilitated by the use of the HCP-MMP atlas (Ekert et al., 2021a). For example, STSdp is implicated in the short-term retention of auditory representations that can be derived from either auditory or visual inputs. The left Peri-Sylvian Language (PSL) region may hold auditory representations of expected speech on-line until the spoken output is matched to the intended speech. TPOJ1 was not implicated in auditory or phonological short-term memory, but more in motor tasks (Ekert et al., 2021a).

Group 2. TGv 44 45 47l SFL 55b.

The above provides the context for the Group 2 regions and network, which are likely to be involved in speech processing, which include regions 44, 45 and 47l with the strongly linked TGv. One other region in Group 2 is 55b, which is situated in the premotor cortex sandwiched between the frontal eye fields FEF and PEF (Fig. 1) (Glasser et al., 2016a). 55b is likely to be an output region for 44 and 45 (Fig. 3), and may be especially important in vocalization and articulation given the importance of vocal cord control in speech production (Ekert et al., 2021b). An alternative is that 55b is involved in the control of eye movements that is especially important in reading. Similarly, the Superior Frontal Language area (SFL) also part of Group 2 may be a supplementary premotor cortical area involved in speech production. The involvement of 47l and 47s in the inferior frontal gyrus regions linked by effective connectivity with language systems is found here in the context of left hemisphere functions. These orbital parts of the language system may be involved in retrieving articulatory plans from semantic stimuli (i.e., semantic-to-articulatory recoding) (Ekert et al., 2021b). The left inferior frontal sulcus (IFS) regions found here to have connectivity with the Group 2 regions may be involved in similar functions (Ekert et al., 2021b). In the right hemisphere the corresponding 47l and 47s regions may be able to function more as lateral orbitofrontal areas involved in non-reward, punishment, and emotion, and consistent with this, functional connectivities and activations related to emotion computations are more prominent in the right hemisphere (Cheng et al., 2016; Rolls et al., 2020c, 2020b, 2020a).

The present investigation extends previous concepts about Broca's area (Amunts and Zilles, 2012; Clos et al., 2013), by showing that there is a whole group of interconnected areas in the frontal lobe of the left hemisphere that are implicated in language, not only regions 44 and 45 in the HCP-MMP atlas (which may not correspond exactly to BA44 and BA45), but also IFSp and IFJa, and 47l and 47s. Similarly, the concept of a Wernicke's area involved in speech comprehension at the temporo-parietal junction is no longer accepted (DeWitt and Rauschecker, 2013; Binder, 2017), but the concept here is that there is a semantic system that extends from the temporal pole to PGi (and PF for body including somatosensory representations (Rolls et al., 2022a)) in the

parietal lobe, which in the temporal lobe has an inferior more visual and object-related part (Group 1), and a more superior auditory/visual motion/somatosensory related part (Group 3). Region 45 has more effective connectivity with STS regions than does region 44 (Figs. 2 and 3). Parts of the supramarginal part of the parietal lobe (which include PF regions) are implicated in auditory short-term memory and articulatory sequencing (Oberhuber et al., 2016). Parts of the angular gyrus of the parietal lobe (which include PG regions) are implicated in semantic processing involved for example in comprehension when reading (Seghier et al., 2010). It should be noted that the inferior STS (Group 1) and superior STS (Group 3) temporal lobe semantic systems identified here by their connectivity do not correspond to the ventral and dorsal auditory pathways in which a ventral pathway is involved in 'what' and a dorsal pathway in 'where' or action processing (Tian et al., 2001; Rauschecker and Scott, 2009; DeWitt and Rauschecker, 2013; Rauschecker, 2018a; Archakov et al., 2020).

It is noted that Broca's area, BA44 and BA45, is no longer thought to be essential for speech production in terms of articulation as shown by the analysis of effects of damage to it (Gajardo-Vidal et al., 2021), but is implicated in some aspects of language, such as the timing of speech items (Long et al., 2016), and syntax as set out below (Friederici et al., 2017).

4.1. Multimodal semantic representations

So far, the emphasis has been on visual and auditory semantic representations, partly because 'what' visual and auditory processing, which is primarily about the external world, is performed in the temporal lobes. However, some neurons in the cortex in the macaque superior temporal sulcus do respond to somatosensory stimuli (Baylis et al., 1987). Even the parietal PGi system considered here is at least dominated by visual system connectivity (Rolls et al., 2022a), and what seems to be missing so far in the PGi part of this system, is information about the somatosensory properties of objects, and how the objects can be manipulated, perhaps as tools, under somatosensory as well as visual control. Now of course any information from the somatosensory system is quite different in kind from what is represented in the temporal lobes, for the somatosensory system involves touch to the body or the position of the body, which is not a property that needs to be taken into account by the temporal lobe analysis of objects 'out there' in the world. The way is which somatosensory information is incorporated into semantic systems appears to be implemented using the Group 3 regions which have effective connectivity with somatosensory regions (frontal opercular FOP, insula and parietal PF). Consistent with this, the Group 3 regions such as STV receive inputs from posterior cingulate cortex region PCV (Fig. 2) which is in the visuo-motor part of the posterior cingulate cortex (Rolls et al., 2022d), and this may enable inputs involved in visually-guided reaching to grasp for objects, with the grasping part of the action requiring somatosensory input to complete the action, to be incorporated into semantic representations of objects.

A key region for multimodal convergence is the set of temporo-parieto-occipital junction regions TPOJ1-3, which are highly connected with each other (Figs. 2 and 3), and which between them have effective connectivities with all the major systems just described, including visual, auditory, STS, PF, and PGi (Rolls et al., 2022a). The implication is that in terms of connectivity the TPOJ2 and TPOJ3 regions both of which have connectivity with the Group 3 regions (Figs. 2 and 3) contribute to bringing together semantic representations involving all of these types of representation in the brain. Further, the Group 3 region PSL, the Peri-Sylvian Language region, receives effective connectivity from PF (Fig. 2) which can be considered as the top of the somatosensory hierarchy (Rolls et al., 2022a). Another input to the TPOJ regions comes from the cortex just lateral to the fusiform face area, which is the visual word-form area (VWFA) (Dehaene et al., 2005; Dehaene and Cohen, 2011; Yeatman and White, 2021; Caffarra et al., 2021). Disruption of the connectivity of the VWFA is likely to account for problems such as alexia and dyslexia in which the visual analysis required for reading cannot reach the semantic TPO regions (Pritchard et al., 2018; Liuzzi et al., 2019). Indeed, the FFC has effective connectivity to TPOJ1 and TPOJ2 and to the superior temporal visual area (STV) which in turn connects strongly with the nearby TPOJ regions. Further, PHT, lateral to the FFC, projects to TPOJ2.

The temporal pole TG regions of the cortex are also likely to form multimodal 'semantic' representations, but primarily based on visual and auditory properties of objects, which is what are represented in the temporal lobes.

The ways in which inputs reach these semantic brain regions in the temporal lobes and temporo-parieto-occipital junction regions from different specialized areas, and the subtypes of sensory modality in which each part of the semantic system appears to specialize as described here in terms of connectivity, not only provides a connectomic basis for the semantic maps that can be visualized using natural speech as inputs (Huth et al., 2016), but also provides a connectional basis for understanding the many dissociations between syndromes found in neuropsychology, including phonological vs visual-based impairments of language processing. Indeed, the connectivity described here is consistent with evidence that the inferior parietal cortex is involved in language-based semantic processing and phonological operations (Coslett and Schwartz, 2018). In this context, it has been suggested that the parietal cortex is involved in the transcoding of sound-based representations into a format that can drive action systems (Coslett and Schwartz, 2018). Although there is much debate about how different language functions may map to different brain regions, one recent study tested patients with strokes in different brain regions, and found some evidence that damage to the posterior middle temporal gyrus is associated with syntactic comprehension deficits; that damage to the posterior inferior frontal gyrus is associated with expressive agrammatism; and that damage to the inferior angular gyrus is associated with semantic category word fluency deficits (Matchin et al., 2022), consistent with a theoretical proposal (Matchin and Hickok, 2020).

The effective connectivity algorithm used here can reveal indirect effects where there may be no direct connections between cortical areas revealed with diffusion tractography, with examples that Fig. 6 provides no indication of direct connections between STS regions and Group 1 regions 10v 9m 10pp 47s 8Av 8BL 9a 9p; and similarly, the tractography did not reveal connections between the temporal lobe regions of Group 1 and inferior prefrontal cortical areas, so these may be indirect effects. So in this respect the effective connectivity measured by the present Hopf algorithm may be useful. At the same time, the Hopf effective connectivity algorithm is non-linear, and indicates effective connectivities only for the links with higher functional connectivities (see further in the Supplementary Material). An implication appears to be that the Hopf effective connectivity algorithm at least as used here does reflect evidence about causal effects between regions that does not in practice extend far across a system of potentially connected areas, and in this respect is more specific and selective than what is typically shown by functional connectivity which can reflect many indirect interactions, again at least with the threshold used here. The power of the Hopf effective connectivity algorithm as used here is emphasised by the selectivity of the connectivity with contralateral cortical areas (Figs. S2 and S3), which is strongest for corresponding cortical regions in the contralateral hemisphere which are correctly identified by the algorithm. The effective connectivity algorithm of course goes far beyond functional connectivity measurements by showing directional effects, which are especially interesting for the language systems as shown in Fig. 4. It is noted that the analyses performed here were of resting state (sometimes termed task-free) brain activity, in which language was not being heard or spoken, though language systems in the brain were likely to be active. It will be of great interest in future research and probably very revealing to investigate how the effective connectivity described here changes during the performance of different types

of syntactic, semantic, phonological, reading, and speech production tasks.

4.2. Relation of the language networks and brain regions described here to previous investigations

The Group 2 network described here involving outputs from other language regions to areas 44, 45 and a closely connected inferior frontal gyrus region including IFja and IFSp, and extending into left orbitofrontal 47s and 47l is suggested here to be involved in syntax, with the syntactic processing (Rolls and Deco, 2015) being driven by semantic inputs from the Group 1 inferior STS temporal lobe visual object 'what' semantic network and the Group 3 superior STS temporal lobe visual motion / auditory / somatosensory semantic network. Consistent with this, there is evidence from neuroimaging and related neuropsychological studies that implicates area 44 in syntax processing, manipulating and detecting structures above the word level (Friederici et al., 2017; Hertrich et al., 2020). In more detail, area 44 is seen as the key region for syntactic processing by implementing the 'merge' operation that is key for understanding syntax (Friederici et al., 2017). Merge is an operation that takes exactly two (syntactic) elements — call them x and y — and puts them together to form the unordered set $[x,y]$ (Friederici et al., 2017). The elements x and y can be word-like building blocks that are drawn from the lexicon or previously constructed phrases that are assembled into an unbounded array of hierarchically structured internal representations (phrases and, ultimately, sentences) (Friederici et al., 2017). Merge is a recursive operation, but as analyzed by Treves and Rolls (1994), in the brain recurrent processing could be implemented by an equivalent series of linked networks. Area 45 is described as a lexical-semantic core area linking phonological codes to lexical meanings (Friederici et al., 2017; Hertrich et al., 2020).

An anterior part of the superior temporal lobe (in Group 3) is identified as an auditory word form area (DeWitt and Rauschecker, 2013; Binder, 2015, 2017; Hertrich et al., 2020). A more posterior part of the superior temporal lobe in the superior temporal gyrus is involved in auditory-phonological processing (Hertrich et al., 2020), consistent with the auditory connectivity described here. Just inferior to that in posterior parts of the superior temporal gyrus, superior temporal sulcus, and middle temporal gyrus is a region implicated in 'syntax and semantics' (Hertrich et al., 2020). This is probably close to the temporo-parieto-occipital junction region (part of Group 3) the connectivity of which is shown in Fig. 7b.

Regions in the more inferior part of the STS and linked with inferior temporal cortex visual regions in Group 1 are implicated in "semantic representations involved in speech, reading, and visual and supramodal mental objects that are linked to word forms" (Hertrich et al., 2020)". The temporo-parietal junction and angular gyrus regions in Group 1 are implicated in "pragmatic processing, context integration, words with multiple meanings, perspective taking, and social cognition" (Hertrich et al., 2020), consistent with some of the points made above about the regions in the Group 1 network.

In a different approach seed-based functional connectivity provided evidence for a dorsal articulatory-phonological network involving inferior frontal and supramarginal regions; a ventral semantic network involving anterior middle temporal and angular gyri; a speech perception network involving superior temporal and sensorimotor regions; and a network between posterior inferior temporal and intraparietal regions linking visual, phonological, and attentional processes for written language (Battistella et al., 2020).

It may be remarked here that if neuroimaging studies could be mapped into a single atlas such as the HCP-MMP atlas using the tools that are available (Glasser et al., 2016a; Dickie et al., 2019; Huang et al., 2022), this would help in the development of our understanding of language systems, especially now that the connectivity between these language-related regions is becoming better understood, as described here.

5. Conclusions

The effective connectivity described here provides evidence for two partly separated semantic networks.

The first semantic network (Group 1) in the inferior parts of the STS / temporal lobe and PG visual parts of the inferior parietal cortex incorporates information from temporal pole TG, ventral temporal visual 'what' regions, some auditory-related regions (e.g., A5 and parts of the STS), medial orbitofrontal / vmPFC / anterior cingulate cortex reward value / emotional regions, and parietal PG (angular gyrus) mainly visual regions (Rolls et al., 2022a), and frontal pole, and has connectivity with the hippocampal episodic memory system via the posterior parts of the posterior cingulate cortex that are related to episodic memory (Rolls et al., 2022d). This system may therefore specialize in visual and auditory 'what' representations and their reward-related meaning. These representations are typically of objects outside the body, viewed or heard in external space.

A second semantic network (Group 3) involves more superior parts of the temporal lobe including the superior STS regions and auditory cortex regions, the somatosensory parietal PF region, some visual areas with motion-related activity (MT, MST), and the visuo-motor part of the posterior parietal cortex. This network includes and has connectivity with a core set of regions near the temporo-parietal junction including TPOJ1-3, the PeriSylvian Language area and the Superior Temporal Visual (STV) region. This semantic system is thereby implicated in semantic representations of the body, and of visuomotor events close to the body involved in actions in nearby space, and in dynamically changing stimuli including those involving the face, vocalization and other auditory stimuli. This system may thereby be involved in representations of the self, and its social relations to others. These two semantic systems may have links with each other in the cortex in the STS and temporal pole (Fig. 2).

What the two partly different semantic systems have in common are strong effective connectivity directed to the Group 2 network which includes regions 44 and 45 (Broca's area), which may perform the mapping from semantic representations to temporally organised and syntactic speech and language (Rolls and Deco, 2015), and which has onward connections to premotor 55b and the Superior Frontal Language region (SFL).

Funding

The research was supported by the following grants to Professor J. Feng: National Key R&D Program of China (No. 2019YFA0709502); 111 Project (No. B18015); Shanghai Municipal Science and Technology Major Project (No. 2018SHZDZX01), ZJLab, and Shanghai Center for Brain Science and Brain-Inspired Technology; and National Key R&D Program of China (No. 2018YFC1312904). G.D. is supported by a Spanish national research project (Ref. PID2019-105772GB-I00 MCIU AEI) funded by the Spanish Ministry of Science, Innovation and Universities (MCIU), State Research Agency (AEI); HBP SGA3 Human Brain Project Specific Grant Agreement 3 (grant agreement No. 945539), funded by the EU H2020 FET Flagship programme; SGR Research Support Group support (Ref. 2017 SGR 1545), funded by the Catalan Agency for Management of University and Research Grants (AGAUR); Neurotwin Digital twins for model-driven non-invasive electrical brain stimulation (grant agreement ID: 101017716) funded by the EU H2020 FET Proactive programme; euSNN European School of Network Neuroscience (grant agreement ID: 860563) funded by the EU H2020 MSCA-ITN Innovative Training Networks; CECH The Emerging Human Brain Cluster (Id. 001-P-001682) within the framework of the European Research Development Fund Operational Program of Catalonia 2014-2020; Brain-Connects: Brain Connectivity during Stroke Recovery and Rehabilitation (Id. 201725.33) funded by the Fundacio La Marato TV3; Corticity, FLAG-ERA JTC 2017, (Ref. PCI2018-092891) funded by the

Spanish Ministry of Science, Innovation and Universities (MCIU), State Research Agency (AEI).

Ethical permissions

No data were collected as part of the research described here. The data were from the Human Connectome Project, and the WU-Minn HCP Consortium obtained full informed consent from all participants, and research procedures and ethical guidelines were followed in accordance with the Institutional Review Boards (IRB), with details at the HCP website http://www.humanconnectome.org/

Data and code availability

The data are available at the HCP website http://www.humanconnectome.org/. Code for the Hopf effective connectivity algorithm is available at https://www.github.com/decolab/Effective-Connectivity–Hopf.

Declaration of Competing Interest

The authors have no competing interests to declare.

Acknowledgments

The neuroimaging data were provided by the Human Connectome Project, WU-Minn Consortium (Principal Investigators: David Van Essen and Kamil Ugurbil; 1U54MH091657) funded by the 16 NIH Institutes and Centers that support the NIH Blueprint for Neuroscience Research; and by the McDonnell Center for Systems Neuroscience at Washington University. Roscoe Hunter of the University of Warwick is thanked for contributing to the description in the Supplementary Material of the Hopf effective connectivity algorithm.

Supplementary materials

Supplementary material associated with this article can be found, in the online version, at doi:10.1016/j.neuroimage.2022.119352.

References

Amunts, K., Zilles, K., 2012. Architecture and organizational principles of Broca's region. Trends Cogn. Sci. 16, 418–426.
Arcaro, M.J., Livingstone, M.S., 2021. On the relationship between maps and domains in inferotemporal cortex. Nat. Rev. Neurosci. 22, 573–583.
Archakov, D., De Witt, I., Kusmierek, P., Ortiz-Rios, M., Cameron, D., Cui, D., Morin, D.L., VanMeter, J.W., Sama, M., Jaaskelainen, I.P., Rauschecker, J., 2020. Auditory representation of learned sound sequences in motor regions of the macaque brain. Proc Natl Acad Sci U S A 117, 15242–15252. doi:10.1073/pnas.1915610117.
Baddeley, A.D., 2021. Developing the concept of working memory: the role of neuropsychology. Arch. Clin. Neuropsychol. 36, 861–873.
Bajaj, S., Adhikari, B.M., Friston, K.J., Dhamala, M., 2016. Bridging the gap: dynamic causal modeling and granger causality analysis of resting state functional magnetic resonance imaging. Brain Connect. 6, 652–661.
Battistella, G., Borghesani, V., Henry, M., Shwe, W., Lauricella, M., Miller, Z., Deleon, J., Miller, B.L., Dronkers, N., Brambati, S.M., Seeley, W.W., Mandelli, M.L., Gorno-Tempini, M.L., 2020. Task-free functional language networks: reproducibility and clinical application. J. Neurosci. 40, 1311–1320.
Baylis, G.C., Rolls, E.T., Leonard, C.M., 1987. Functional subdivisions of the temporal lobe neocortex. J. Neurosci. 7, 330–342.
Bellot, E., Abassi, E., Papeo, L., 2021. Moving toward versus away from another: how body motion direction changes the representation of bodies and actions in the visual cortex. Cereb. Cortex 31, 2670–2685.
Binder, J.R., 2015. The Wernicke area: modern evidence and a reinterpretation. Neurology 85, 2170–2175.
Binder, J.R., 2017. Current controversies on Wernicke's area and its role in language. Curr. Neurol. Neurosci. Rep. 17, 58.
Booth, M.C.A., Rolls, E.T., 1998. View-invariant representations of familiar objects by neurons in the inferior temporal visual cortex. Cereb. Cortex 8, 510–523.
Bornkessel-Schlesewsky, I., Schlesewsky, M., Small, S.L., Rauschecker, J.P., 2015. Neurobiological roots of language in primate audition: common computational properties. Trends Cogn. Sci. 19, 142–150.
Bouchard, K.E., Mesgarani, N., Johnson, K., Chang, E.F., 2013. Functional organization of human sensorimotor cortex for speech articulation. Nature 495, 327–332.
Buckner, R.L., DiNicola, L.M., 2019. The brain's default network: updated anatomy, physiology and evolving insights. Nat. Rev. Neurosci. 20, 593–608.
Caffarra, S., Karipidis, II, Yablonski, M., Yeatman, J.D., 2021. Anatomy and physiology of word-selective visual cortex: from visual features to lexical processing. Brain Struct. Funct. 226, 3051–3065.
Cai, X., Padoa-Schioppa, C., 2012. Neuronal encoding of subjective value in dorsal and ventral anterior cingulate cortex. J. Neurosci. 32, 3791–3808.
Chang, E.F., Raygor, K.P., Berger, M.S., 2015. Contemporary model of language organization: an overview for neurosurgeons. J. Neurosurg. 122, 250–261.
Cheng, W., Rolls, E.T., Qiu, J., Liu, W., Tang, Y., Huang, C.C., Wang, X., Zhang, J., Lin, W., Zheng, L., Pu, J., Tsai, S.J., Yang, A.C., Lin, C.P., Wang, F., Xie, P., Feng, J., 2016. Medial reward and lateral non-reward orbitofrontal cortex circuits change in opposite directions in depression. Brain 139, 3296–3309.
Clos, M., Amunts, K., Laird, A.R., Fox, P.T., Eickhoff, S.B., 2013. Tackling the multifunctional nature of Broca's region meta-analytically: co-activation-based parcellation of area 44. Neuroimage 83, 174–188.
Collins, J.A., Olson, I.R., 2014. Beyond the FFA: The role of the ventral anterior temporal lobes in face processing. Neuropsychologia 61, 65–79.
Coslett, H.B., Schwartz, M.F., 2018. The parietal lobe and language. Handb. Clin. Neurol. 151, 365–375.
Critchley, H., Daly, E., Phillips, M., Brammer, M., Bullmore, E., Williams, S., Van Amelsvoort, T., Robertson, D., David, A., Murphy, D., 2000. Explicit and implicit neural mechanisms for processing of social information from facial expressions: a functional magnetic resonance imaging study. Hum. Brain Mapp. 9, 93–105.
Davis, S.W., Wing, E.A., Cabeza, R., 2018. Contributions of the ventral parietal cortex to declarative memory. Handb. Clin. Neurol. 151, 525–553.
Deco, G., Cabral, J., Woolrich, M.W., Stevner, A.B.A., van Hartevelt, T.J., Kringelbach, M.L., 2017a. Single or multiple frequency generators in on-going brain activity: a mechanistic whole-brain model of empirical MEG data. Neuroimage 152, 538–550.
Deco, G., Kringelbach, M.L., Jirsa, V.K., Ritter, P., 2017b. The dynamics of resting fluctuations in the brain: metastability and its dynamical cortical core. Sci. Rep. 7, 3095.
Deco, G., Cruzat, J., Cabral, J., Tagliazucchi, E., Laufs, H., Logothetis, N.K., Kringelbach, M.L., 2019. Awakening: predicting external stimulation to force transitions between different brain states. Proc. Natl. Acad. Sci. 116, 18088–18097.
Dehaene, S., Cohen, L., Sigman, M., Vinckier, F., 2005. The neural code for written words: a proposal. Trends Cogn. Sci. 9, 335–341.
Dehaene, S., Cohen, L., 2011. The unique role of the visual word form area in reading. Trends Cogn. Sci. 15, 254–262.
Dere, E., Easton, A., Nadel, L., Huston, J.P., 2008. Handbook of Episodic Memory. Elsevier, Amsterdam.
DeWitt, I., Rauschecker, J.P., 2013. Wernicke's area revisited: parallel streams and word processing. Brain Lang. 127, 181–191.
Dickie, E.W., Anticevic, A., Smith, D.E., Coalson, T.S., Manogaran, M., Calarco, N., Viviano, J.D., Glasser, M.F., Van Essen, D.C., Voineskos, A.N., 2019. Ciftify: a framework for surface-based analysis of legacy MR acquisitions. Neuroimage 197, 818–826.
Ding, N., Melloni, L., Zhang, H., Tian, X., Poeppel, D., 2016. Cortical tracking of hierarchical linguistic structures in connected speech. Nat. Neurosci. 19, 158–164.
DiNicola, L.M., Braga, R.M., Buckner, R.L., 2020. Parallel distributed networks dissociate episodic and social functions within the individual. J. Neurophysiol. 123, 1144–1179.
Ekert, J.O., Gajardo-Vidal, A., Lorca-Puls, D.L., Hope, T.M.H., Dick, F., Crinion, J.T., Green, D.W., Price, C.J., 2021a. Dissociating the functions of three left posterior superior temporal regions that contribute to speech perception and production. Neuroimage 245, 118764.
Ekert, J.O., Lorca-Puls, D.L., Gajardo-Vidal, A., Crinion, J.T., Hope, T.M.H., Green, D.W., Price, C.J., 2021b. A functional dissociation of the left frontal regions that contribute to single word production tasks. Neuroimage 245, 118734.
Ekstrom, A.D., Ranganath, C., 2018. Space, time, and episodic memory: The hippocampus is all over the cognitive map. Hippocampus 28, 680–687.
Elston, G.N., Benavides-Piccione, R., Elston, A., Zietsch, B., Defelipe, J., Manger, P., Casagrande, V., Kaas, J.H., 2006. Specializations of the granular prefrontal cortex of primates: implications for cognitive processing. Anat. Rec. Part A Discov. Mol. Cell. Evol. Biol. 288, 26–35.
Elston, G.N., 2007. Specializations in pyramidal cell structure during primate evolution. In: Kaas, J.H., Preuss, T.M. (Eds.), Evolution of Nervous Systems. Academic Press, Oxford, pp. 191–242.
Finzi, D., Gomez, J., Nordt, M., Rezai, A.A., Poltoratski, S., Grill-Spector, K., 2021. Differential spatial computations in ventral and lateral face-selective regions are scaffolded by structural connections. Nat. Commun. 12, 2278.
Frassle, S., Lomakina, E.I., Razi, A., Friston, K.J., Buhmann, J.M., Stephan, K.E., 2017. Regression DCM for fMRI. Neuroimage 155, 406–421.
Freiwald, W.A., 2020. The neural mechanisms of face processing: cells, areas, networks, and models. Curr. Opin. Neurobiol. 60, 184–191.
Freyer, F., Roberts, J.A., Becker, R., Robinson, P.A., Ritter, P., Breakspear, M., 2011. Biophysical mechanisms of multistability in resting-state cortical rhythms. J. Neurosci. 31, 6353–6361.
Freyer, F., Roberts, J.A., Ritter, P., Breakspear, M., 2012. A canonical model of multistability and scale-invariance in biological systems. PLoS Comput. Biol. 8, e1002634.
Friederici, A.D., Chomsky, N., Berwick, R.C., Moro, A., Bolhuis, J.J., 2017. Language, mind and brain. Nat. Hum. Behav. 1, 713–722.
Friston, K., 2009. Causal modelling and brain connectivity in functional magnetic resonance imaging. PLoS Biol. 7, e33.
Gajardo-Vidal, A., Lorca-Puls, D.L., Team, P., Warner, H., Pshdary, B., Crinion, J.T., Leff, A.P., Hope, T.M.H., Geva, S., Seghier, M.L., Green, D.W., Bowman, H., Price, C.J., 2021. Damage to Broca's area does not contribute to long-term speech production outcome after stroke. Brain 144, 817–832.
Geschwind, N., 1970. The organization of language and the brain. Science 170, 940–944.

Gilbert, S.J., Burgess, P.W., 2008. Executive function. Curr. Biol. 18, R110–R114.
Gilson, M., Moreno-Bote, R., Ponce-Alvarez, A., Ritter, P., Deco, G., 2016. Estimation of directed effective connectivity from fMRI functional connectivity hints at asymmetries in the cortical connectome. PLoS Comput. Biol. 12, e1004762.
Glasser, M.F., Sotiropoulos, S.N., Wilson, J.A., Coalson, T.S., Fischl, B., Andersson, J.L., Xu, J., Jbabdi, S., Webster, M., Polimeni, J.R., Van Essen, D.C., Jenkinson, M.Consortium, W.U.-M.H., 2013. The minimal preprocessing pipelines for the Human Connectome Project. Neuroimage 80, 105–124.
Glasser, M.F., Coalson, T.S., Robinson, E.C., Hacker, C.D., Harwell, J., Yacoub, E., Ugurbil, K., Andersson, J., Beckmann, C.F., Jenkinson, M., Smith, S.M., Van Essen, D.C., 2016a. A multi-modal parcellation of human cerebral cortex. Nature 536, 171–178.
Glasser, M.F., Smith, S.M., Marcus, D.S., Andersson, J.L., Auerbach, E.J., Behrens, T.E., Coalson, T.S., Harms, M.P., Jenkinson, M., Moeller, S., Robinson, E.C., Sotiropoulos, S.N., Xu, J., Yacoub, E., Ugurbil, K., Van Essen, D.C., 2016b. The human connectome project's neuroimaging approach. Nat. Neurosci. 19, 1175–1187.
Goldman-Rakic, P.S., 1996. The prefrontal landscape: implications of functional architecture for understanding human mentation and the central executive. Philos. Trans. R. Soc. B 351, 1445–1453.
Grabenhorst, F., Rolls, E.T., 2011. Value, pleasure, and choice in the ventral prefrontal cortex. Trends Cogn. Sci. 15, 56–67.
Griffanti, L., Salimi-Khorshidi, G., Beckmann, C.F., Auerbach, E.J., Douaud, G., Sexton, C.E., Zsoldos, E., Ebmeier, K.P., Filippini, N., Mackay, C.E., Moeller, S., Xu, J., Yacoub, E., Baselli, G., Ugurbil, K., Miller, K.L., Smith, S.M., 2014. ICA-based artefact removal and accelerated fMRI acquisition for improved resting state network imaging. Neuroimage 95, 232–247.
Hagoort, P., Indefrey, P., 2014. The neurobiology of language beyond single words. Annu. Rev. Neurosci. 37, 347–362.
Hagoort, P., 2017. The core and beyond in the language-ready brain. Neurosci. Biobehav. Rev. 81, 194–204.
Hasselmo, M.E., Rolls, E.T., Baylis, G.C., 1989a. The role of expression and identity in the face-selective responses of neurons in the temporal visual cortex of the monkey. Behav. Brain Res. 32, 203–218.
Hasselmo, M.E., Rolls, E.T., Baylis, G.C., Nalwa, V., 1989b. Object-centred encoding by face-selective neurons in the cortex in the superior temporal sulcus of the the monkey. Exp. Brain Res. 75, 417–429.
Hertrich, I., Dietrich, S., Ackermann, H., 2020. The margins of the language network in the brain. Front. Commun. 5, 519955.
Hickok, G., Poeppel, D., 2007. The cortical organization of speech processing. Nat. Rev. Neurosci. 8, 393–402.
Hickok, G., Poeppel, D., 2015. Neural basis of speech perception. Handb. Clin. Neurol. 129, 149–160.
Huang, C.-C., Rolls, E.T., Hsu, C.-C.H., Feng, J., Lin, C.-P., 2021. Extensive cortical connectivity of the human hippocampal memory system: beyond the "what" and "where" dual-stream model. Cereb. Cortex 31, 4652–4669.
Huang, C.C., Rolls, E.T., Feng, J., Lin, C.P., 2022. An extended human connectome project multimodal parcellation atlas of the human cortex and subcortical areas. Brain Struct. Funct. 227, 763–778.
Huth, A.G., de Heer, W.A., Griffiths, T.L., Theunissen, F.E., Gallant, J.L., 2016. Natural speech reveals the semantic maps that tile human cerebral cortex. Nature 532, 453–458.
Kaas, J.H., Hackett, T.A., 2000. Subdivisions of auditory cortex and processing streams in primates. Proc. Nat. Acad. Sci. USA 97, 11793–11799.
Kanwisher, N., McDermott, J., Chun, M.M., 1997. The fusiform face area: a module in human extrastriate cortex specialized for face perception. J. Neurosci. 17, 4302–4311.
Kelly, C., Uddin, L.Q., Shehzad, Z., Margulies, D.S., Castellanos, F.X., Milham, M.P., Petrides, M., 2010. Broca's region: linking human brain functional connectivity data and non-human primate tracing anatomy studies. Eur. J. Neurosci. 32, 383–398.
Kemmerer, D., 2015. Cognitive Neuroscience of Language. Psychology Press, New York.
Kringelbach, M.L., McIntosh, A.R., Ritter, P., Jirsa, V.K., Deco, G., 2015. The rediscovery of slowness: exploring the timing of cognition. Trends Cogn. Sci. 19, 616–628.
Kringelbach, M.L., Deco, G., 2020. Brain states and transitions: insights from computational neuroscience. Cell Rep. 32, 108128.
Kuznetsov, Y.A., 2013. Elements of Applied Bifurcation Theory. Springer Science & Business Media, New York.
Leech, R., Sharp, D.J., 2014. The role of the posterior cingulate cortex in cognition and disease. Brain 137, 12–32.
Leech, R., Smallwood, J., 2019. The posterior cingulate cortex: Insights from structure and function. Handb. Clin. Neurol. 166, 73–85.
Lehky, S.R., Tanaka, K., 2016. Neural representation for object recognition in inferotemporal cortex. Curr. Opin. Neurobiol. 37, 23–35.
Liuzzi, A.G., Bruffaerts, R., Vandenberghe, R., 2019. The medial temporal written word processing system. Cortex 119, 287–300.
Long, M.A., Katlowitz, K.A., Svirsky, M.A., Clary, R.C., Byun, T.M., Majaj, N., Oya, H., Howard, M.A., Greenlee, J.D.W., 2016. Functional segregation of cortical regions underlying speech timing and articulation. Neuron 89, 1187–1193.
Maravita, A., Romano, D., 2018. The parietal lobe and tool use. Handb. Clin. Neurol. 151, 481–498.
Markov, N.T., Vezoli, J., Chameau, P., Falchier, A., Quilodran, R., Huissoud, C., Lamy, C., Misery, P., Giroud, P., Ullman, S., Barone, P., Dehay, C., Knoblauch, K., Kennedy, H., 2014. Anatomy of hierarchy: feedforward and feedback pathways in macaque visual cortex. J. Comp. Neurol. 522, 225–259.
Matchin, W., Hickok, G., 2020. The cortical organization of syntax. Cereb. Cortex 30, 1481–1498.
Matchin, W., Basilakos, A., Ouden, D.D., Stark, B.C., Hickok, G., Fridriksson, J., 2022. Functional differentiation in the language network revealed by lesion-symptom mapping. Neuroimage 247, 118778.
Milton, C.K., Dhanaraj, V., Young, I.M., Taylor, H.M., Nicholas, P.J., Briggs, R.G., Bai, M.Y., Fonseka, R.D., Hormovas, J., Lin, Y.H., Tanglay, O., Conner, A.K., Glenn, C.A., Teo, C., Doyen, S., Sughrue, M.E., 2021. Parcellation-based anatomic model of the semantic network. Brain Behav. 11, e02065.
Moscovitch, M., Cabeza, R., Winocur, G., Nadel, L., 2016. Episodic memory and beyond: the hippocampus and neocortex in transformation. Annu. Rev. Psychol. 67, 105–134.
Oberhuber, M., Hope, T.M.H., Seghier, M.L., Parker Jones, O., Prejawa, S., Green, D.W., Price, C.J., 2016. Four Functionally Distinct Regions in the Left Supramarginal Gyrus Support Word Processing. Cereb. Cortex 26, 4212–4226.
Padoa-Schioppa, C., Conen, K.E., 2017. Orbitofrontal cortex: A neural circuit for economic decisions. Neuron 96, 736–754.
Papagno, C., 2018. Memory deficits. Handbook of clinical neurology. Parietal Cortex 151, 377–393.
Perrett, D., Mistlin, A., Chitty, A., 1987. Visual neurons responsive to faces. Trends Neurosci. 10, 358–364.
Perrett, D.I., Rolls, E.T., Caan, W., 1982. Visual neurons responsive to faces in the monkey temporal cortex. Exp. Brain Res. 47, 329–342.
Pitcher, D., Ungerleider, L.G., 2021. Evidence for a third visual pathway specialized for social perception. Trends Cogn. Sci. 25, 100–110.
Pritchard, S.C., Coltheart, M., Marinus, E., Castles, A., 2018. A computational model of the self-teaching hypothesis based on the dual-route cascaded model of reading. Cogn. Sci. 42, 722–770.
Rauschecker, J.P., Tian, B., Hauser, M., 1995. Processing of complex sounds in the macaque nonprimary auditory cortex. Science 268, 111–114.
Rauschecker, J.P., 1998. Cortical processing of complex sounds. Curr. Opin. Neurobiol. 8, 516–521.
Rauschecker, J.P., Scott, S.K., 2009. Maps and streams in the auditory cortex: nonhuman primates illuminate human speech processing. Nat. Neurosci. 12, 718–724.
Rauschecker, J.P., 2012. Ventral and dorsal streams in the evolution of speech and language. Front. Evol. Neurosci. 4, 7.
Rauschecker, J.P., 2018a. Where, when, and how: are they all sensorimotor? Towards a unified view of the dorsal pathway in vision and audition. Cortex 98, 262–268.
Rauschecker, J.P., 2018b. Where did language come from? Precursor mechanisms in non-human primates. Curr. Opin. Behav. Sci. 21, 195–204.
Razi, A., Seghier, M.L., Zhou, Y., McColgan, P., Zeidman, P., Park, H.J., Sporns, O., Rees, G., Friston, K.J., 2017. Large-scale DCMs for resting-state fMRI. Netw. Neurosci. 1, 222–241.
Reber, J., Feinstein, J.S., O'Doherty, J.P., Liljeholm, M., Adolphs, R., Tranel, D., 2017. Selective impairment of goal-directed decision-making following lesions to the human ventromedial prefrontal cortex. Brain 140, 1743–1756.
Rolls, E.T., 1984. Neurons in the cortex of the temporal lobe and in the amygdala of the monkey with responses selective for faces. Hum. Neurobiol. 3, 209–222.
Rolls, E.T., Treves, A., Tovee, M.J., 1997a. The representational capacity of the distributed encoding of information provided by populations of neurons in the primate temporal visual cortex. Exp. Brain Res. 114, 177–185.
Rolls, E.T., Treves, A., Tovee, M.J., Panzeri, S., 1997b. Information in the neuronal representation of individual stimuli in the primate temporal visual cortex. J. Comput. Neurosci. 4, 309–333.
Rolls, E.T., 2000. Functions of the primate temporal lobe cortical visual areas in invariant visual object and face recognition. Neuron 27, 205–218.
Rolls, E.T., Treves, A., 2011. The neuronal encoding of information in the brain. Prog. Neurobiol. 95, 448–490.
Rolls, E.T., 2014. Emotion and Decision-Making Explained. Oxford University Press, Oxford.
Rolls, E.T., Deco, G., 2015. Networks for memory, perception, and decision-making, and beyond to how the syntax for language might be implemented in the brain. Brain Res. 1621, 316–334.
Rolls, E.T., 2016. Cerebral Cortex: Principles of Operation. Oxford University Press, Oxford.
Rolls, E.T., 2018. The storage and recall of memories in the hippocampo-cortical system. Cell Tissue Res. 373, 577–604.
Rolls, E.T., 2019a. The Orbitofrontal Cortex. Oxford University Press, Oxford.
Rolls, E.T., 2019b. The cingulate cortex and limbic systems for emotion, action, and memory. Brain Struct. Funct. 224, 3001–3018.
Rolls, E.T., 2020. Neural computations underlying phenomenal consciousness: a higher order syntactic thought theory. Front. Psychol. (Conscious. Res.) 11, 655.
Rolls, E.T., Cheng, W., Du, J., Wei, D., Qiu, J., Dai, D., Zhou, Q., Xie, P., Feng, J., 2020a. Functional connectivity of the right inferior frontal gyrus and orbitofrontal cortex in depression. Soc. Cogn. Affect. Neurosci. 15, 75–86.
Rolls, E.T., Cheng, W., Feng, J., 2020b. The orbitofrontal cortex: reward, emotion, and depression. Brain Commun. 2, fcaa196.
Rolls, E.T., Vatansever, D., Li, Y., Cheng, W., Feng, J., 2020c. Rapid rule-based reward reversal and the lateral orbitofrontal cortex. Cereb. Cortex Commun. 1. doi:10.1093/texcom/tgaa1087.
Rolls, E.T., 2021a. Brain Computations: What and How. Oxford University Press, Oxford.
Rolls, E.T., 2021b. The neuroscience of emotional disorders. In: Heilman, K.M., Nadeau, S.E. (Eds.), Handbook of Clinical Neurology: Disorders of Emotion in Neurologic Disease. Elsevier, Oxford, pp. 1–26.
Rolls, E.T., 2021c. Learning invariant object and spatial view representations in the brain using slow unsupervised learning. Front. Comput. Neurosci. 15, 686239.
Rolls, E.T., 2021d. Mind causality: a computational neuroscience approach. Front. Comput. Neurosci. 15, 70505.
Rolls, E.T., Deco, G., Huang, C.C., Feng, J., 2022a. The human posterior parietal cortex: effective connectome, and its relation to function. Cereb. Cortex in review in revision.
Rolls, E.T., Deco, G., Huang, C.C., Feng, J., 2022b. The effective connectivity of the human hippocampal memory system. Cereb. Cortex doi:10.1093/cercor/bhab1442.

Rolls, E.T., Deco, G., Huang, C.C., Feng, J., 2022c. The human orbitofrontal cortex, vmPFC, and anterior cingulate cortex effective connectome: emotion, memory, and action. Cereb. Cortex doi:10.1093/cercor/bhac1070.

Rolls, E.T., Wirth, S., Deco, G., Huang, C.C., Feng, J., 2022d. The human posterior cingulate cortex effective connectome, and implications for memory and navigation.

Rubinov, M., Sporns, O., 2010. Complex network measures of brain connectivity: uses and interpretations. Neuroimage 52, 1059–1069.

Salimi-Khorshidi, G., Douaud, G., Beckmann, C.F., Glasser, M.F., Griffanti, L., Smith, S.M., 2014. Automatic denoising of functional MRI data: combining independent component analysis and hierarchical fusion of classifiers. Neuroimage 90, 449–468.

Satterthwaite, T.D., Elliott, M.A., Gerraty, R.T., Ruparel, K., Loughead, J., Calkins, M.E., Eickhoff, S.B., Hakonarson, H., Gur, R.C., Gur, R.E., Wolf, D.H., 2013. An improved framework for confound regression and filtering for control of motion artifact in the preprocessing of resting-state functional connectivity data. Neuroimage 64, 240–256.

Schurz, M., Tholen, M.G., Perner, J., Mars, R.B., Sallet, J., 2017. Specifying the brain anatomy underlying temporo-parietal junction activations for theory of mind: A review using probabilistic atlases from different imaging modalities. Hum. Brain Mapp. 38, 4788–4805.

Seghier, M.L., Fagan, E., Price, C.J., 2010. Functional subdivisions in the left angular gyrus where the semantic system meets and diverges from the default network. J. Neurosci. 30, 16809–16817.

Shallice, T., Burgess, P., 1996. The domain of supervisory processes and temporal organization of behaviour. Philos. Trans. R. Soc. B 351, 1405–1411.

Shallice, T., Cipolotti, L., 2018. The prefrontal cortex and neurological impairments of active thought. Annu. Rev. Psychol. 69, 157–180.

Smith, S.M., Beckmann, C.F., Andersson, J., Auerbach, E.J., Bijsterbosch, J., Douaud, G., Duff, E., Feinberg, D.A., Griffanti, L., Harms, M.P., Kelly, M., Laumann, T., Miller, K.L., Moeller, S., Petersen, S., Power, J., Salimi-Khorshidi, G., Snyder, A.Z., Vu, A.T., Woolrich, M.W., Xu, J., Yacoub, E., Ugurbil, K., Van Essen, D.C., Glasser, M.F.Consortium, W.U.M.H., 2013. Resting-state fMRI in the human connectome project. Neuroimage 80, 144–168.

Tian, B., Reser, D., Durham, A., Kustov, A., Rauschecker, J.P., 2001. Functional specialization in rhesus monkey auditory cortex. Science 292, 290–293.

Treves, A., Rolls, E.T., 1994. A computational analysis of the role of the hippocampus in memory. Hippocampus 4, 374–391.

Underwood, A.G., Guynn, M.J., Cohen, A.L., 2015. The future orientation of past memory: the role of BA 10 in prospective and retrospective retrieval modes. Front. Hum. Neurosci. 9, 668.

Valdes-Sosa, P.A., Roebroeck, A., Daunizeau, J., Friston, K., 2011. Effective connectivity: influence, causality and biophysical modeling. Neuroimage 58, 339–361.

van der Linden, M., Berkers, R.M.W.J., Morris, R.G.M., Fernandez, G., 2017. Angular gyrus involvement at encoding and retrieval is associated with durable but less specific memories. J. Neurosci. 37, 9474–9485.

Van Essen, D.C., Smith, S.M., Barch, D.M., Behrens, T.E., Yacoub, E., Ugurbil, K.Consortium, W.U.-M.H., 2013. The WU-minn human connectome project: an overview. Neuroimage 80, 62–79.

Vann, S.D., Aggleton, J.P., Maguire, E.A., 2009. What does the retrosplenial cortex do? Nat. Rev. Neurosci. 10, 792–802.

Yeatman, J.D., White, A.L., 2021. Reading: the confluence of vision and language. Annu. Rev. Vis. Sci. 7, 487–517.